Available online at www.sciencedirect.com

SCIENCE DIRECT®

Organic Geochemistry 37 (2006) 688–710

Organic Geochemistry

www.elsevier.com/locate/orggeochem

Organic geochemical characterization of a Miocene core sample from Haughton impact structure, Devon Island, Nunavut, Canadian High Arctic

Lorraine B. Eglinton [a,*], Darlene Lim [b], Greg Slater [c], Gordon R. Osinski [d], Jean K. Whelan [a], Marianne Douglas [e]

[a] *Department of Marine Chemistry and Geochemistry, Woods Hole Oceanographic Institution, Woods Hole, MA 02543, USA*
[b] *NASA Ames Research Center, Building 245, Mail-Stop 245-3, Moffett Field, CA 94035-1000, USA*
[c] *School of Geography and Geology, 1280 Main Street West, McMaster University, Hamilton, Ont., Canada L8S 4K1*
[d] *Canadian Space Agency, 6767 Route de l'Aeroport, Saint-Hubert, Que., Canada J3Y 8Y9*
[e] *Department of Geology, 22 Russell Street, University of Toronto, Toronto, Ont., Canada M5S 3B1*

Received 30 December 2004; received in revised form 25 April 2005; accepted 10 January 2006
Available online 18 April 2006

Abstract

Extremely well preserved sedimentary deposits in the Haughton impact structure (HIS) provide a unique record of the post-impact Miocene lacustrine depositional environment. Detailed organic geochemical characterization of a hydrocarbon-impregnated band found in a core from the crater-lake sedimentary infill reveals a complex source history for the hydrocarbons. These include contributions from eroded pre- and post-impact formations together with inputs from contemporaneous flora and fauna, a deep, possibly lower Paleozoic petroleum as well as a contribution from hydrothermally altered organic biopolymers. Geochemical data coupled with paleolimnology and geology proves to be a valuable tool for studying the provenance of hydrocarbons associated with the HIS and can give insights, not only into the post-impact geology, but also into processes that may contribute to the generation of petroleum fluids at other impact sites.

1. Introduction

Impact craters have been a focus of significant study in recent years due to their potential as sources of petroleum and ore deposits. At least 25% of the currently known impact craters worldwide are associated with various economic deposits (Grieve and Masaytis, 1994). Impact craters have been considered to be both potentially good sources and good reservoirs for petroleum fluids, in particular. For example, the Steen River impact crater, Alberta, is ~25 km in diameter, ~97.5 Ma old and produces approximately 1000 barrels of oil per day with a gas production approaching 35 million cubic feet per day from rim structures resulting from impact (Mazur et al., 2000). While impact events generally do not produce hydrocarbons, the

---

[*] Corresponding author. Fax: +1 508 457 2164.
E-mail address: leglinton@whoi.edu (L.B. Eglinton).

0146-6380/$ - see front matter © 2006 Elsevier Ltd. All rights reserved.
doi:10.1016/j.orggeochem.2006.01.006

resultant structures provide favorable conditions for hydrocarbon migration (i.e. fractured, faulted, and brecciated target rocks), and form basins in which post-impact sediments can accumulate if conditions are favorable. These intra-crater sedimentary rocks can potentially act as hydrocarbon source rocks and/or cap rocks, depending on the conditions of deposition, and subsequent geological evolution.

Devon Island in the Canadian High Arctic is the site of a ~39 Ma old terrestrial impact crater. This ~23 km diameter crater is currently under much investigation as an analogy for geological features on Mars (e.g. Lee et al., 1998). Of the approximately 170 impact craters known to exist at the present time (Earth Impact Database, 2004), the Devon Island crater is one of the best exposed and best preserved. The crater itself is known as the Haughton impact structure (HIS). Palaentological and paleolimnological studies have proposed the existence of a post-impact lake, near the center of the crater that was subsequently in-filled with a series of sediments now characterized as the Haughton Formation (Hickey et al., 1988). The development of an impact-associated hydrothermal system has also been documented at the HIS (Osinski et al., 2001). Fluid flow would likely have been enhanced in the crater due to the formation of impact derived fractures and fissures and listric faulting. The impact was determined by Jessburger (1988) to have occurred at 23 Ma; however, recent findings by Osinski and Lee (personal communication) suggest that a significant period of post impact erosional activity occurred before the Haughton Formation was deposited and this supports new data from Sherlock et al. (personal communication) dating the impact some 16 Ma older.

Sectioning of a core from the HIS revealed an unusual 1 cm thick band that had a strong hydrocarbon odor. This paper reports on the geochemical characterization of this band and its possible origins. Studying the provenance of hydrocarbons associated with the HIS can give insights, not only into the post-impact geology, but also into processes that may contribute to generation of petroleum fluids at other impact sites.

2. Geological setting

Haughton (75°22′ N, 89°40′ W) is a sub-circular impact structure ~23 km in diameter that impacted lower Paleozoic shelf-type sediments that overlie a gneissic Precambrian basement in the western sector of Devon Island, Nunavut, Canadian Archipelago (Thorsteinsson and Mayr, 1987) (Fig. 1). The ~1.8 km thick Ordovician-Silurian sedimentary sequence is dominated by carbonates, with minor evaporites, sandstones, and shales (Thorsteinsson and Mayr, 1987). These formations are unconformably overlain by up to ~125 m of what has been deemed lithic or fragmental impact breccia by Redeker and Stöffler (1988), or carbonate-rich impact melt breccias by Osinski and Spray (2001, 2003). Shocked basement gneisses from Haughton have been estimated at 23.4 ± 1.0 Ma through ^{40}Ar–^{39}Ar dating (Jessburger, 1988). However, more recent studies (Osinski and Lee, personal communication) coupled with high precision laserprobe ^{40}Ar–^{39}Ar dating by Sherlock et al. (personal communication) suggest the Haughton Formation significantly postdates the impact event, at 39 ± 2 Ma which is consistent with an early Miocene age for the Haughton Formation.

The Haughton Formation, which overlies the carbonate-rich impact melt hills in certain areas, is composed of up to 48 m of interbedded dolomite-rich lacustrine silt, fine sand and mud (Hickey et al., 1988). These lacustrine deposits contain a rich assemblage of pollen, plant macrofossils, and the only known record of early Neogene arctic vertebrates (Whitlock and Dawson, 1990). *Pinus, Picea, Tsuga, Larix, Betula, Alnus*, and *Corylus* pollen were found to be the most abundant pollen types represented in the Haughton lacustrine remains (Hickey et al., 1988; Whitlock and Dawson, 1990), and are comparable to modern-day pollen distributions associated with mixed conifer-hardwood forests of eastern coastal North America. Gramineae pollen are entirely absent from the deposit, suggesting an early Miocene date for the Haughton Formation. The Late Cretaceous to Eocene Eureka Sound Group was apparently not present in the area at the time of impact but is found 30 km north of the HIS. Here the group is 210 m thick and rests unconformably on the Silurian rocks (Hickey et al., 1988) of the Grinnell Peninsula (Fig. 1).

3. Experimental

3.1. Sample collection

Detailed coring information can be found in the DRILLEX report produced by Schutt et al. (2002), and as such an abbreviated description is included in this section. Coring systems and sam-

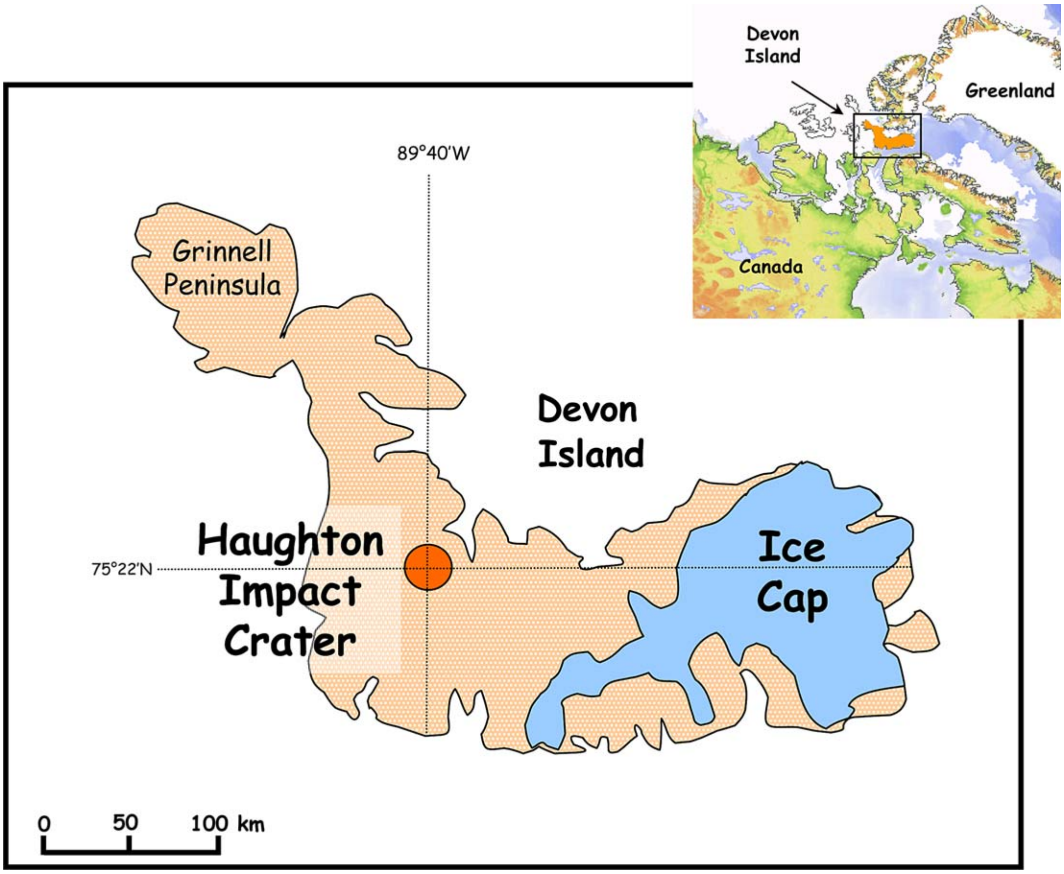

Fig. 1. Location map of Haughton impact structure, Devon Island, Nunavut, Canadian Arctic archipelago showing the extent of the ice cap. (After Robertson, 1988).

plers were loaned by the US Army Corps of Engineers Cold Regions Research and Engineering Laboratory (CRREL). Specifically, a JK Smit GW-15 Winkie drill, along with a variety of CRREL coring augers were used in the exercise. Drill cores were procured without the use of fluids/lubricants to offset costs, to minimize environmental impacts, and to lessen the chance of sample contamination. Through this method the Haughton-Mars Project (HMP) DRILLEX program extracted seven cores from the Haughton Formation of varying lengths (2.35 m–6.71 m) over the period of June 29th–July 11th, 1998. These were coded Auger Hole (AH) 98-1 to AH98-7. A total of 24.46 m of core length was recovered from these seven boreholes.

Once the cores were retrieved, they were immediately wrapped in plastic liners and stored in an ice chest containing dry ice for shipment to the NASA Ames Research Center, CA, where they were stored in a −20 °C cold-room.

A detailed list of these labeled sections, their corresponding depths and other pertinent subsampling information can be found in Lim (2004). A brief summary of procedures is provided as follows. Core AH98-3 (75°23′48.930″N, 89°48′54.210″W) was selected for diatom microfossil analysis given that it was the longest, and most complete core recovered from the Haughton Formation (Lim, 2004). The core had been recovered in 12 subsections, totaling 6.71 m in length. These were alphabetized from the top down (i.e. sections A–H, then J–M; a section of H was initially mislabeled as section I, which is why the latter is now excluded from the list).

Sub-sampling and archiving of core AH98-3 was conducted on-site at the NASA Ames Research Center by D. Lim and M. Douglas in late May 2001. Each frozen core section was halved using a Gryphon diamond band saw, photographed, and both halves labeled then wrapped in cellophane wrap and aluminum foil. The archival halves were returned to the Ames freezer and the working portions were subsequently shipped to the University of Toronto, Department of Geology and stored in a freezer.

In order to identify areas of stratigraphic interest, the non-archival sections of core AH98-3 were X-radiographed at the Geology Department of Queen's University, Kingston, Ont. Next, the core was sub-sampled every 5 cm. Also, based on the X-ray results, other areas of interest, such as regions of distinct banding, were additionally sub-sampled. These sub-samples were then placed in labeled 15 ml plastic scintillation vials and stored frozen. A small sub-section of the core containing a "hydrocarbon impregnated band" from a core depth of 27–28 cm was shipped frozen to Woods Hole Oceanographic Institution, MA.

3.2. Analytical techniques

3.2.1. Sample preparation

A 3 g wet sample, spiked with a recovery standard (d_{50} *n*-tetracosane, d_{10} phenanthrene, d_{12} 2,6-dimethylnaphthalene), was ultrasonically extracted, using a Tekmar® sonic disrupter, in tandem with a spiked procedural blank. Ultrasonic extraction was performed in pulse mode at a duty cycle of 70% and an output value of 7. The probe was cleaned with sequential rinses of methanol, dichloromethane (DCM) and hexane and then pulsed for 2 min in DCM. Saturated and aromatic hydrocarbons were recovered from the wet sediment using sequential extractions and centrifugations using the following solvent regime: (1) 40 ml of methanol (2) 40 ml of DCM and (3) 40 ml of hexane. The supernatants from each independent extraction were combined into a single flask. The total extracts were reduced by rotary evaporation and then passed through an activated copper column for removal of elemental sulfur. Microcolumn chromatography, using 90% activated silica gel, was used to fractionate the extracts into saturated, aromatic and polar hydrocarbon pools. The fractions were concentrated using rotary evaporation. The concentrate was transferred with DCM to 150 μl glass inserts, followed by gentle evaporation in a stream of nitrogen to near dryness. The fractions were diluted with 100 μl DCM and the sample submitted for chemical and isotopic analysis. All glassware was solvent rinsed and combusted at 450 °C; all solvents were high purity Fischer Scientific MS grade. Dry weight was determined by weighing a homogenized aliquot of sample material; allowing it to dry at 50 °C in an oven overnight and then reweighing.

Before total organic carbon analysis (TOC), a sub-aliquot of ground whole rock sample was transferred to small vials and fumed with HCl to remove any carbonate minerals. The samples were then dried at 50 °C for 48 h. Approximately 35 mg of sample was then weighed in 5 × 8 mm ultra-clean tin capsules. The samples were then analyzed for carbon on a CE Instruments Flash 1112 Series EA CHN analyzer with a sequence of standards and blanks.

3.2.2. Gas chromatography–mass spectrometry (GC–MS)

Biological marker distributions were obtained using gas chromatography coupled with mass specific detection using the saturated and aromatic hydrocarbon fractions. A Hewlett Packard (HP) 6890 gas chromatograph fitted with a Restek® DB-5 MS 60 m glass capillary column and connected directly to an HP 5963 mass specific detector was used. After cool on-column injection the gas chromatograph was programmed from 50 °C to 325 °C at a rate of 3 °C/min and held at 325 °C for 20 min. The mass spectrometer was operated in EI-mode at 70 eV in selected ion monitoring mode. A total of 30 ions characteristic of *n*-alkane, sterane, terpane, aromatic steroid, aromatic hydrocarbons and other target ions specific to higher plant material were monitored in two sequential runs. Table 1 lists target ions. Full mass spectra (50–550 amu) were recorded on the saturated and aromatic fractions to identify less common biological markers. Compounds were identified by their key fragmentation ions based on relative retention times and comparison with published data (e.g. Mackenzie, 1980, 1984; Philp, 1985).

3.2.3. Isotope-ratio-monitoring gas chromatography–mass spectrometry (irmGC–MS)

Compound specific carbon isotope analysis was performed on the saturated fraction on an irmGC–MS system consisting of an HP 6890 interfaced to a Finnigan-MAT DeltaPlus via a GC Combustion III interface. The GC was equipped with a CP-Sil 5CB column (50 m × 0.25 mm i.d. × 0.25 μm phase thickness). Samples were injected into a Gerstel CIS (PTV) injector at 10 °C, held for 0.25 min, ramped at 12 °C/s to 350 °C, held for 3 min. The GC temperature program was 60 °C, held for

Table 1
List of target compounds analyzed by GC–MSD

Target compounds	Monitoring ions
Steranes	217
14β,17β(H)-Steranes	218
n-Alkanes	57, 85, 99
Benzothiophenes	134, 148, 162, 176
Phenanthrenes	178, 192, 206, 220
Dibenzothiophenes	184, 198
Demethylated triterpanes	177
Triterpanes	191
Methylated triterpanes	205
Mono-aromatic steroids	253
Tri-aromatic steroids	231
Isonorpimarane, Norpimarane	233, 123, 109
Fichtelite	109, 95, 81
Pimarane	247, 163, 123
α- and ββ-Phyllocladane	259, 231, 123
Calamenene	159
5,6,7,8-Tetrahydrocadalene	187, 159
Cadalene	183, 168, 153
Dehydroabietane	255, 173, 159
Simonellite	237, 195, 179
Retene	219, 204
Ferruginol	271, 201, 189
Primaranes and isoprimaranes	272, 276, 302

3 min, ramped at 20 °C/min to 130 °C, ramped at 3 °C/min up to 260 °C ramped at 10 °C/min up to 340 °C, held for 2 min.

3.2.4. Organic petrological screening and vitrinite reflectance determination

A small sub-aliquot of crushed whole rock was prepared for petrological analysis in accordance with ICCP (1963, 1971, 1975) protocols. The crushed particles were subsequently mounted in a small hole drilled in a solid resin block. A small amount of epoxy resin (Struers Serifix®) was added to cold set the particles in the block. The set sample was ground and polished using an automated Buehler Ecomet 3®, with an Automet 2® head, polishing system. The sample was ground sequentially using 240, 400, 600, 1200 carborundum papers and isopropanol as lubricant. After each grinding stage the sample was washed with alcohol to remove debris and prevent swelling.

Three polishing laps covered with Buehler Mastertex® short-nap cloth were loaded with alumina powders of decreasing grain size and used in the following sequence: 1 μm, 0.3 μm and 0.05 μm. Isopropanol was used as a lubricant during polishing. After each polishing the sample was washed in alcohol to remove debris. Finally, the block was hand-buffed to remove fine smears and checked under a microscope for polish quality and particle relief.

Vitrinite reflectance determination was performed in a dark-room using a Zeiss Standard Universal research microscope-photometer system (MPM01K) equipped with a tungsten-halogen lamp (12 V, 100 W), at 40× Epiplan oil immersion objective, filtered 546 nm incident light and Zeiss immersion oil (n_e 1.517 at 23 °C). The pinhole measuring diaphragm was set to 2 μm diameter and a lamp field stop reduced interfering reflectances during measurement.

Glass and mineral standards of known reflectance were used for calibration. A Zeiss triple glass standard with reflectances of 0.506%, 1.025% and 1.817% was used in addition to M^{c}Crone® yttrium-aluminum-garnet (0.927%), spinel (0.418%) and cubic zirconium (3.287%) standards. The standards were kept in dust free boxes at constant temperature and humidity prior to use. Random reflectance measurements were made (i.e. no rotation of the microscope stage) in non-polarized light. Data were acquired using a Zeiss PMI-2, interfaced for computer data acquisition and processing. Photometer linearity tests were performed using all six standards and vitrinite analysis was conducted only if the correlation coefficient was $\geqslant$0.999. Three standards were measured, each in triplicate on different spots on the standard surface, at the beginning of the analysis and every 30 min during analyses.

4. Results

4.1. Extract yields

The extractable organic matter yield corrected for recovery and dry sediment weight is rather low at 19 μg/g. The calculated procedural recovery (based on internal standard response) was 85%. *n*-Alkane distributions are based on the highest yields approximating 7.1 ppm followed by the hopanes present at 1.6 ppm and then the naphthalenes at 0.46 ppm. Sterane yields are considerably lower at 22 ppb; anything below 1 ppb was considered unreliable. Biomarker yields were calculated based on internal standards and mass spectra. Hopane abundance is 70-fold greater than sterane abundance in the Haughton extract. Total organic carbon (TOC) measured on extracted rock is low at <0.3%.

4.2. Acyclic biomarkers

The total ion current (TIC) is dominated by *n*-alkanes showing a strong contribution of long-chain C_{20+} hydrocarbons. An envelope starting at *n*-C_{12} extends out to *n*-C_{42} with a maximum at *n*-C_{27}, typical of high wax oils, and a subtle elevation at *n*-C_{17}, typical of algal input. Hydrocarbons with carbon chain lengths shorter than *n*-C_{20} are present in lesser amounts. Isoprenoids pristane and phytane are present in trace amounts. There is a very slight odd over even carbon chain length predominance with a carbon preference index of 1.10. Fig. 2 shows the typical distribution for *n*-alkanes from the *m*/*z* 57 fragmentogram. The lack of any significant odd over even carbon predominance together with the *n*-alkane carbon range indicates the hydrocarbons have reached the beginning of catagenesis in thermal terms, probably early oil window mature, and indicate a possible contribution from vascular plant waxes.

The mature *n*-alkane distribution, using traditional interpretation, implies a large contribution from waxy terrestrial material. However, Fowler (1984) proposed an alternative interpretation for Ordovician oils, attributing the longer-chain *n*-alkanes as products derived from bacterial membrane lipids. Interestingly, cyclic alkanes that are also thought to indicate the presence of bacteria in a source depocenter are not detected in abundance in the Haughton extract. Additionally, a number of studies of torbanites show an *n*-alkane envelope of long-chain alkanes with a smooth distribution and negligible abundances of cyclic terpenoids in extracts (Douglas et al., 1969; Largeau et al., 1986; Robinson et al., 1989).

4.3. Cyclic biomarkers

4.3.1. Hopanes

The hopanes are present in much greater abundance (>70*x*) than the steranes. Figure 3 shows the distribution of methylated triterpanes (*m*/*z* 191) for the HIS extract. The most prominent peak in the distribution is the $C_{30}\alpha\beta$ hopane. Tricyclic terpanes are present in trace, ranging to minor abundances compared to longer chained moretanes and homohopanes. The ratio of tricyclic terpanes/

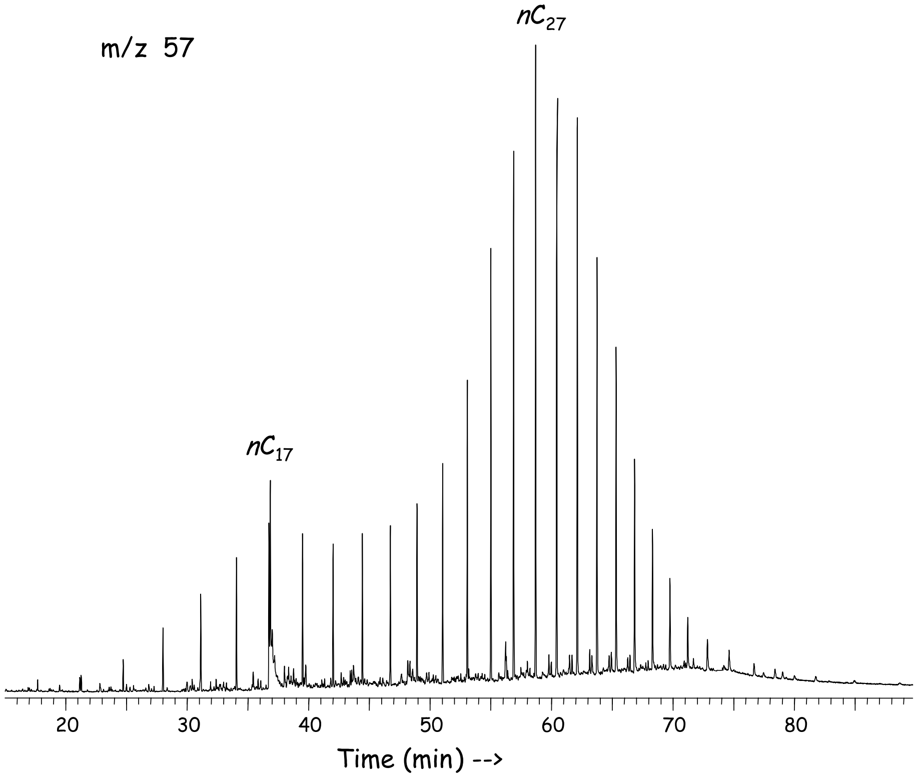

Fig. 2. Distribution of *n*-alkanes from the *m*/*z* 57 mass chromatogram in the Haughton extract.

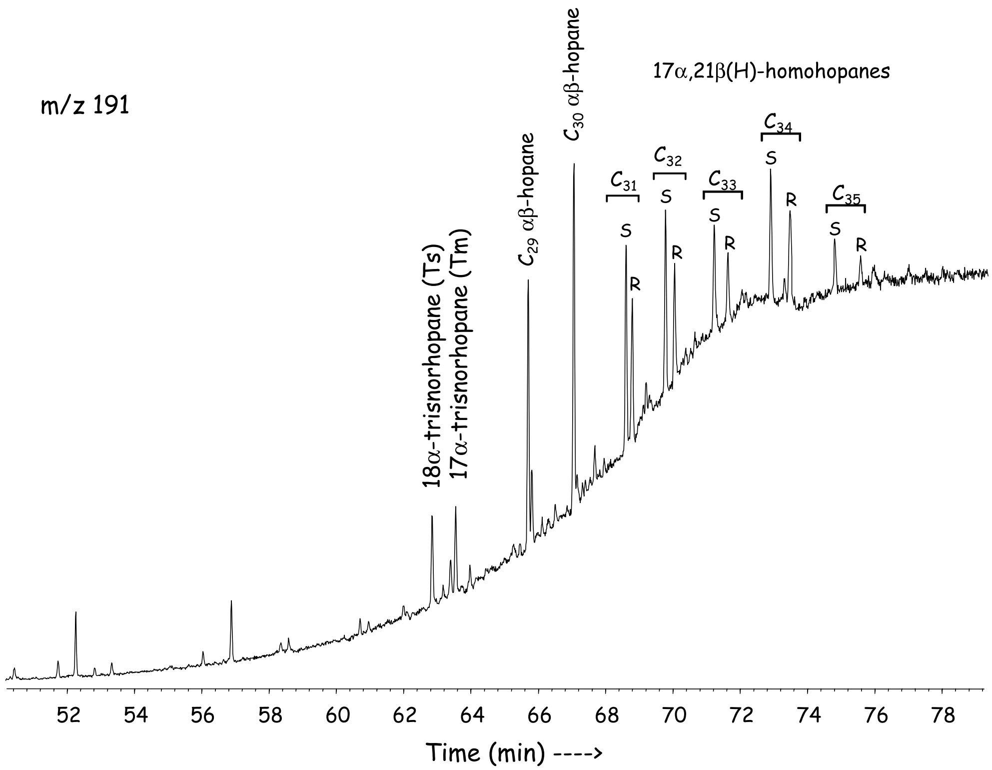

Fig. 3. *m*/*z* 191 mass fragmentogram showing the distributions of terpanes in the Haughton extract.

17α,21β(H)-hopanes has been used to indicate the abundances of bacterial or algal lipids relative to other prokaryotic species (Peters and Moldowan, 1993). However, due to low tricyclic terpane abundance the ratio cannot be accurately measured at Haughton but still implies a predominant prokaryotic biomass. The ratio of C_{27} 18α-22,29,30-trisnorneohopane (Ts)/17α-22,29,30-trisnorhopane (Tm) (Ts/(Ts + Tm)) is 0.52 and represents an equivalent vitrinite reflectance approaching 0.6% indicating early oil window maturity. The epimerisation of the 17α-bishomohopanes at C-22 has reached an equilibrium value of 0.6 (Seifert and Moldowan, 1980) and indicates a thermal maturity of at least 0.6%R_o equivalent, i.e. minimally early oil window and supports the Ts/(Ts + Tm) maturity data. This is typical for the Lower Paleozoic rocks present around and within the Haughton impact structure (Parnell et al., 2003).

The naturally occurring precursors for the hopanoids have the 17β,21β(H) stereochemistry. This biological configuration is very unstable and only present in very immature sediments. The ββ-hopanoids readily convert to βα-moretanes and αβ-hopanes with the latter thermodynamically more stable than the former. The ratio of C_{30}17β, 21α(H)-moretane to the corresponding C_{30}17α, 21β(H)-hopane decreases with increasing thermal maturity. Usually, this ratio decreases from about 0.8 in the immature stage to values of less than 0.15 in the mature stage and to a minimum of 0.05 (Mackenzie, 1980; Seifert and Moldowan, 1980). The moretane to hopane ratio in the Haughton extract has reached a value of 0.09 indicating a minimum level of maturity within the oil window ($\geqslant$0.7%R_o).

The distribution of C_{31}–C_{35} homohopanes in the HIS sample shows elevated C_{34} homohopane in relation to C_{31}–C_{33} homohopanes and depletion of C_{35} homohopane. Homohopanes are thought to originate from bacteriohopanetetrol common in prokaryotic biomass (Rohmer, 1987). They are often used to assess redox potential of marine sediments during diagenesis (Peters and Moldowan, 1991). Elevated C_{33}, C_{34} or C_{35} in relation to lower homologs can indicate highly reducing (low Eh) marine depositional environment (Peters and Moldowan, 1993). These workers also attribute elevated C_{33} or C_{34} as an indication of a different bacterial biomass in the source environment. Enhanced

C_{34} at Haughton may be a manifestation of one lineage of bacteria as yet unidentified or alternatively due to the influence of sulfur in the depositional environment.

Isomerization reactions at the C-22 position for 17α,21β(H)-hopanes are also frequently used molecular proxies of thermal maturity. The biological precursors favor the 22R configuration. The C-22 epimer ratios often increase for the higher homologs. Seifert and Moldowan (1980) determined that the epimer ratios reach thermodynamic equilibrium between values of 0.57–0.62 and these values are indicative of mature hydrocarbons, i.e. the main phase of oil generation has been reached or surpassed (Peters and Moldowan, 1993). C-22 epimer ratios at Haughton indicate a mature oil with values for C_{31}, C_{32} and C_{33} rising linearly from 0.58, 0.60, 0.62, respectively. However, the C_{34} and C_{35} sharply deviate from this trend. C_{35} homohopane indicates a level exceeding equilibrium at 0.77 and may be influenced by co-eluting compounds. C_{34} homohopane epimerization ratio indicates a level of maturity barely entering the oil window (0.53), thereby signifying an immature pattern for what is generally accepted to be a mature homohopane pattern. Biodegradation usually results in selective demethylation of 22R epimers specifically for the C_{34} and C_{35} hopanes (Peters et al., 1996) and thus would preclude an influence from biodegradation to account for the C_{34} homohopane ratio. Alternatively, selective preservation during early diagenesis of sulfur-bound or oxygen-bound (Bishop et al., 1995) homohopane precursors has been associated with elevated C_{35} homohopane under anoxic conditions (Sinninghe Damsté et al., 1995). Köster et al. (1997) demonstrated how natural sulfurisation can influence both carbon number distribution and epimer ratios for homohopanes. These workers show free 17α,21β (H)-hopanes indices from an organic rich marlstone and a dolomite sequence from the Upper Triassic Hauptdolomit Formation (HD) that are remarkably similar to the homohopanes at Haughton in terms of total C_{31} through C_{35}. However, the epimer distribution for the marlstone differs in that it is less mature compared to Haughton. Both these samples show a significant increase in C_{35} epimer ratios resulting from a reduction in C_{35} 22R epimers. The dolomite also shows similarity to the Haughton sample as both exhibit dominant C_{34} homologs. Köster et al. (1997) report a phosphoritic member of the Jurf-ed-Darawish shale (Sinninghe Damsté et al., 1995) that again shows dominant C_{34} homohopanes. They attribute these findings to a more intense degradation of the precursor pentakishomohopanepolyol side chain prior to sulfur incorporation. However, one unique feature of Haughton is that the biologically configured C_{34} 22R isomer is much more prevalent. Thus, while evidence for natural sulfurisation is compelling, it does not fully explain the C_{34} homohopane distributions in the Haughton sample. It may be possible that a bacterially mediated scission of the side chain has occurred. Peters and Moldowan (1991) proposed this can occur under sub-oxic environmental conditions. They give an example of Yugoslavian oil with elevated C_{34} that, with supporting evidence, also infers sub-oxic depositional conditions. However, this sample also shows that C_{34} is dominated by the 22S epimer. It may, therefore, be the case that distributions of the Haughton homohopanes derive from a combination of S-bound hopanoids from a sedimentary rock that was deposited under anoxic–sub-oxic marine conditions with an additional input from more immature hopanoids from contemporaneous bacterial biomass present in deeper zones of the Haughton Formation. Hydrocarbons from both sources have been entrained in a single upward migrating fluid that is now resting in its present location.

Extended C_{32}–C_{36} 2α-methylhopanes are diagnostic for cyanobacteria and prochlorophytes (Bisseret et al., 1985; Summons et al., 1999; Farrimond et al., 2004) while extended C_{32}–C_{36} 3β-methylhopanes may be diagnostic for some microaerophilic proteobacteria (certain methylotrophs, methanotrophs and acetic acid bacteria) (Zundel and Rohmer, 1985a,b,c; Summons and Jahnke, 1992; Farrimond et al., 2004). Trace abundances of homologous series of 2α- and 3β-methylhopanes (*m*/*z* 205) in the Haughton extract are highlighted in Fig. 4. These assignments were based on mass spectra, retention indices and published data (Pancost et al., 1998; Farrimond et al., 2004). Although 2α- and 3β-methylhopanes can derive from a variety of prokaryotes, Summons et al. (1996) and Collister et al. (1992) suggest these biomarkers indicate the presence of cyanobacteria and methylotrophic bacteria, respectively. Isotopic data for the *n*-alkanes range between −29‰ and −31‰ and are not significantly depleted (e.g. −40‰ to −85‰ for methanotrophic bacteria). Unfortunately, resolution was insufficient to determine values for individual hopanes.

The triterpenoid oleanane, a chemical indicator of flowering plants that evolved during Albian times

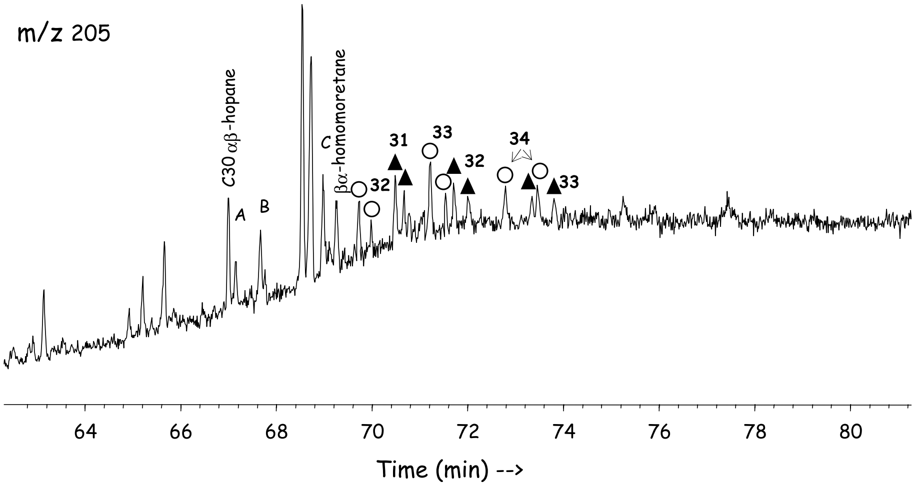

Fig. 4. Distribution of methylhopanes (*m/z* 205) for Haughton impact structure extract. Tentative assignments of 2α-methylhopanes (open circles) and 3β-methylhopanes (solid triangles) are shown. Peak A = 2α-methyl,17α,21β(H)-hopane, peak B = 3β-methyl, 17α,21β(H)-30-norhopane and peak C = 2β-methyl,17α,21β(H)-hopane.

and persists to present day (Ekweozor and Udo, 1988), was targeted but is absent from the Haughton extract. While this could indicate that the hydrocarbons were generated prior to Albian times when angiosperms began to thrive, it may also be an indication of a source with little or no contribution from this type of flora. Gammacerane, a C_{30} triterpane thought to derive from tetrahymanol in both freshwater and marine ciliates was also targeted. When present, gammacerane is indicative of a density stratified water column, a feature often reported in lacustrine and hypersaline depositional environments (ten Haven et al., 1988; Kleemann et al., 1990; Schoell et al., 1994; Sinninghe Damsté et al., 1995). Gammacerane is also absent from the Haughton extract, thereby suggesting a lack of stratification of the water column in the depositional environment.

4.3.2. Diterpenoid hydrocarbons

Several diterpenoids were found in the solvent extract of the Miocene AH98-3 core. In recent plants diterpenoid hydrocarbons are primarily found in gymnosperms with only a few documented occurrences in angiosperms (van Aarssen et al., 1990; Otto et al., 1997). The distribution of non-derivatized diterpenoids in the saturated hydrocarbon fraction of the Haughton extract is dominated by pimarane, isopimarane, abietane and phyllocladane classes (Fig. 5). Structural assignments were made based on key fragmentation ions, relative retention times and comparison with published data (Mackenzie, 1980, 1984; Philp, 1985; Otto et al., 1997; Kalkreuth et al., 1998; Otto and Simoneit, 2001). Fichtelite (norabietane) and isonorpimarane represent a degraded series of diterpenoids with isonorpimarane as the major compound and fichtelite as the minor component of the series. These diterpenoids are interpreted as the diagenetic derivatives of natural product precursors such as abietic and pimaric acids commonly found in extant species of Pinaceae (Thomas, 1970; Otto and Wilde, 2001; Otto and Simoneit, 2002). Since pimarane, isopimarane and abietane classes of diterpenoids are the major components of extant species of Pinaceae it is reasonable to conclude that Pinaceae derived flora are major contributors to the organic matter in Haughton infill sediments. These data are in accordance with botanical assignments made in Hickey et al. (1988), who show palynoflora is dominated by *Pinus and Picea*, sp. Phyllocladane represents a broader origin from other coniferales families (Podocarpaceae, Taxodiaceae, Auraucariaceae and Cupressacea) but is generally not found in the Pinaceae family (Sukh Dev, 1989; Otto et al., 1997). Since the Podocarpaceae, Auraucariaceae and Cupressacea families did not evolve until Late Triassic times and are thought to be restricted to the southern hemisphere, it seems more likely that phyllocladane is related to the Taxodiaceae or Voltziales (Late Carboniferous genesis) families. This, therefore, represents contribution from more than one family of Coniferales into the Haughton sediment and is consistent with mixed gymnosperm forestation.

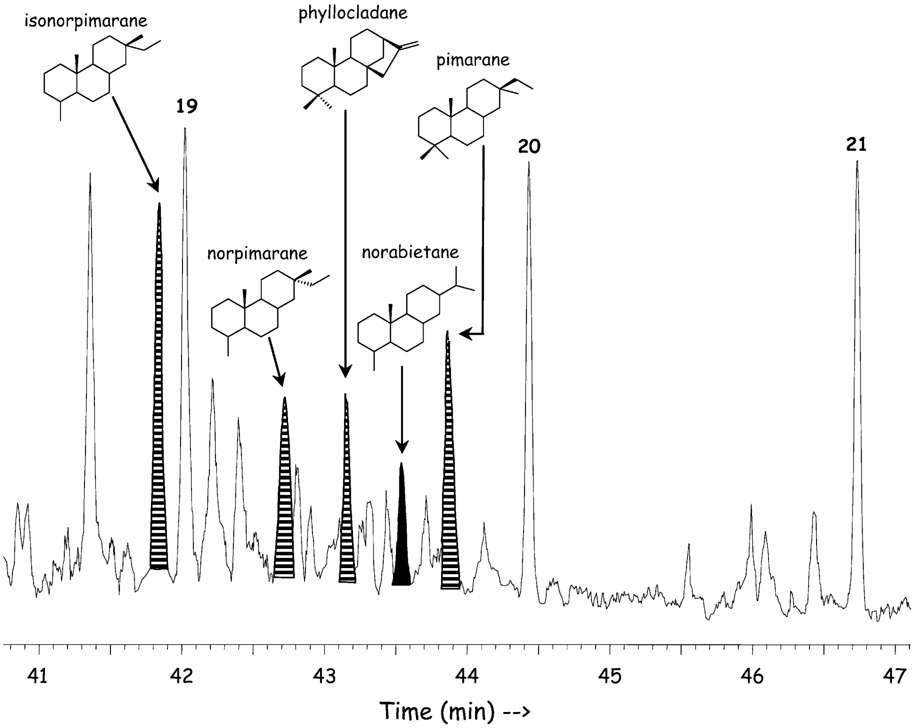

Fig. 5. Total ion current of the saturated hydrocarbon fraction from Haughton impact structure. Diterpenoid hydrocarbon structures representing diagenetic products from plant resins from gymnosperms are highlighted. *n*-Alkanes are labeled by carbon number.

An oxidative diagenetic pathway would lead to the formation of retene, whereas decarboxylation of the natural product abietic acid followed by reduction would result in saturated minor abundances of fichtelite (Otto and Simoneit, 2002). Since retene is absent and minor amounts of fichtelite are present in the Haughton extract, it is reasonable to assume that a reductive, possibly lacustrine, depositional environment may account for the provenance of these compounds in the Haughton sample.

4.3.3. Steranes

Steranes are derived from sterols that are widely dispersed in plants and microorganisms, with the C_{27} and C_{30} sterol precursors most abundant in marine organisms and C_{29} sterols in higher plants for example. Steranes in the HIS extract are present in very low abundances (22 ppb). Fig. 6a shows the distribution of regular steranes from the *m*/*z* 217 mass chromatogram while Fig. 6b shows the distribution of ββ steranes from the *m*/*z* 218 mass chromatogram. Fig. 6b shows the sterane distribution is dominated by C_{29} steranes (60%) followed by the C_{27} steranes (22%) with about 17% accounted for by C_{28} steranes. High percentages of C_{29} steranes indicate a contribution from higher land plants (Huang and Meinschein, 1979; Moldowan et al., 1985). The ratio of regular steranes/17α-hopanes is very low (near zero). This is often used as another independent proxy of terrigenous organic matter input (Moldowan et al., 1985).

Sterane isomerization ratios are used as a proxy for thermal alteration. The 20*S*/(20*S*+20*R*) ratio for regular $C_{29}5\alpha,14\alpha,17\alpha(H)$-steranes is 0.45. Isomerization usually attains equilibrium at 0.55 (Peters and Moldowan, 1993). The ratio of $\beta\beta/(\beta\beta+\alpha\alpha)$ for the 20*S* and 20*R* C_{29} regular steranes is 0.49 (equilibrium 0.70; Peters and Moldowan, 1993). This isomerization is slower to reach equilibrium and appears to be less affected by source than the 20*S*/20*R* sterane ratio. Both ratios indicate a thermal maturity of early oil window.

A series of C_{30} steranes, identified as 24-*n*-propylcholestanes, is present in the Haughton extract. These are thought to be representative of pelagophyte algae, a biomarker for marine conditions, with few exceptions, according to Moldowan et al. (1990). One possible exception exists for an Oligocene sample from a saline lake in the Bohai Basin,

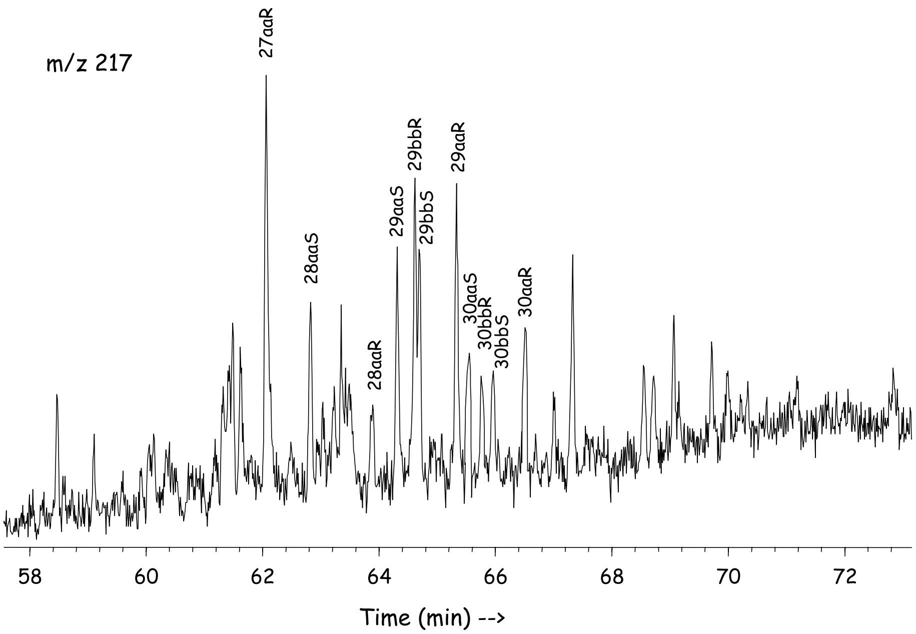

Fig. 6a. Distributions of regular steranes in the Haughton extract from mass chromatogram *m/z* 217. Compound identifications are shown below figure. Figure identifications are as follows:

Code	*Compound*
27aaR	5α,14α,17α(H) (20R) cholestane
28aaS	24-methyl-5α,14α,17α(H) (20S) cholestane
28aaR	24-methyl-5α,14α,17α(H) (20R) cholestane
29aaS	24-ethyl-5α,14α,17α(H) (20S) cholestane
29bbR	24-ethyl-5α,14β,17β(H) (20R) cholestane
29bbS	24-ethyl-5α,14β,17β(H) (20S) cholestane
29aaR	24-ethyl-5α,14α,17α(H) (20R) cholestane
30aaS	24-propyl-5α,14α,17α(H) (20S) cholestane
30bbR	24-propyl-5α,14β,17β(H) (20R) cholestane
30bbS	24-propyl-5α,14β,17β(H) (20S) cholestane
30aaR	24-propyl-5α,14α,17α(H) (20R) cholestane

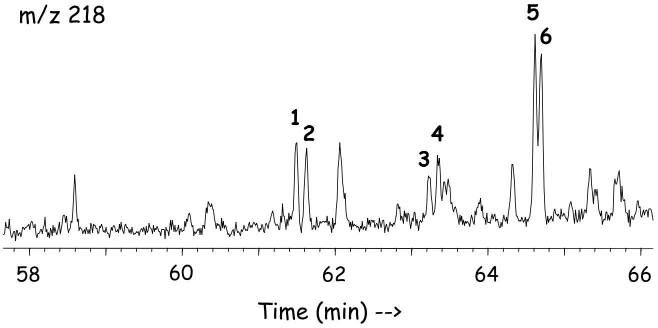

Fig. 6b. Distribution of ββ Steranes from the Haughton extract showing the high abundance of C_{29}ββ steranes. Peak identification is as follows: (1) C_{27}24-methyl-14β,17β(H) cholestane (20*S*); (2) C_{27}24-methyl-14β,17β(H) cholestane (20*R*); (3) C_{28}24-methyl-14β,17β(H) cholestane (20*S*); (4) C_{28}24-methyl-14β,17β(H) cholestane (20*R*); (5) C_{29}24-methyl-14β,17β(H) cholestane (20*S*); (6) C_{29}24-methyl-14β,17β(H) cholestane (20*R*).

China (Moldowan et al., 1990). The algae that biosynthesize the precursors of these C_{30} compounds are thought to have emerged between Ordovician and Devonian times. The 24-*n*-propylcholestanes together with the regular steranes provide evidence for a mixed source for steranes at HIS, one which includes a contribution from a Lower Paleozoic formation such as the Allen Bay Formation, as well as one from more recent reworked terrestrial organic matter.

Rearranged steranes (diasteranes) are below detection levels. The presence of amplified abundances of diasteranes is a good source rock indicator of diagenetic acid-clay catalytic reactions that result in sterane rearrangement via unsaturated intermediates to produce diasteranes. Low abundances of diasteranes at Haughton indicate a clay-starved depositional environment, which is consistent with the carbonate-dominated regional geology.

4.4. Aromatic hydrocarbons

The third most abundant compound group in the Haughton extract is the naphthalenes. Alkylnaphthalenes are prominent compounds in oils and sediment extracts and may be derived from non-aromatic precursors such as terpenoids (Strachan et al., 1988). Fig. 7 shows series of naphthalenes found in the AH98-3 core extract. The methylnaphthalene ratio (MNR) is used as a thermal maturity proxy. In the Haughton extract the MNR is 0.97 and this is equivalent to a higher thermal maturity, approaching 0.89% vitrinite reflectance equivalent (Shimoyama et al., 2000).

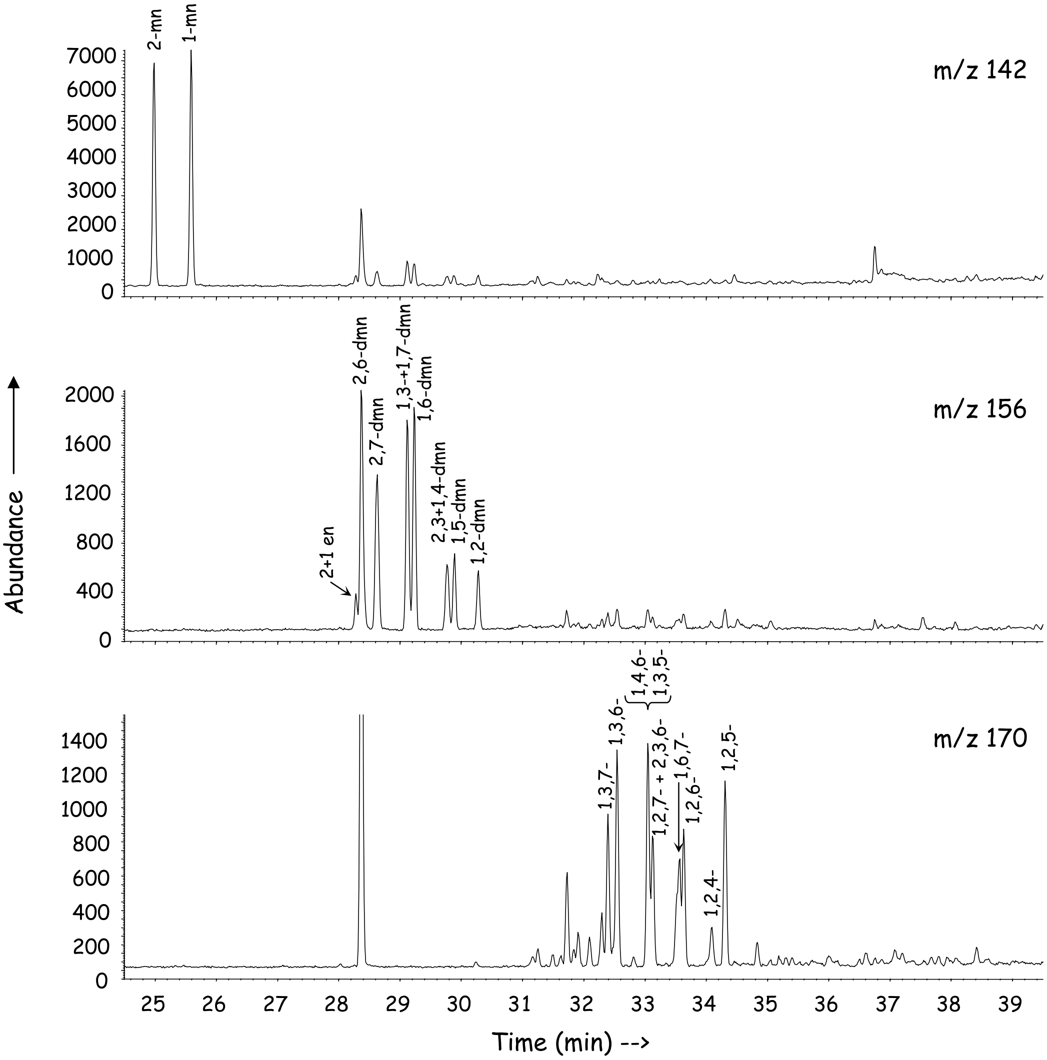

Fig. 7. Distribution of methylnaphthalenes in the Haughton Impact Structure extract.

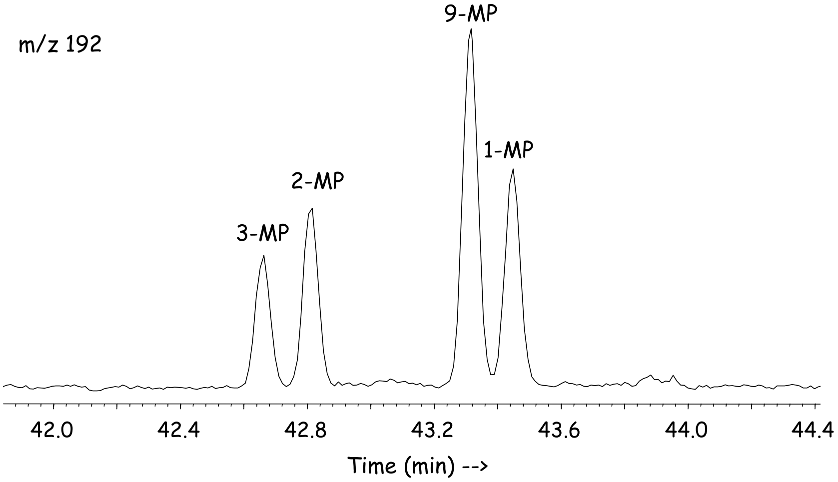

Fig. 8. *m*/*z* 192 mass chromatogram showing the distribution of methylphenanthrenes (MP) in the aromatic hydrocarbon fraction of the Haughton Impact Structure.

Methylphenanthrenes are ubiquitous in petroleum and sediment extracts. Isomer ratios for these methylated aromatics provide good indications of thermal maturity of source rocks (Radke et al., 1982, 1990; Radke and Welte, 1983; Radke, 1988). A nicely resolved suite of methylphenanthrenes in the Haughton extract is shown in Fig. 8. Thermal maturity, based on the methylphenanthrene index 1 (2-methylphenanthrene/1-methylphenanthrene), is 0.47 in the Haughton extract. This translates to an equivalent vitrinite reflectance of 0.70%R_c (Radke, 1988) and represents a thermal maturity within the oil window. Higher alkylated homologues such as cadalene, simonellite and retene were not detected in the Haughton sample.

Monoaromatics steroids are below detection limits in the Haughton extract. However, there is a significant abundance of triaromatic steroidal hydro-

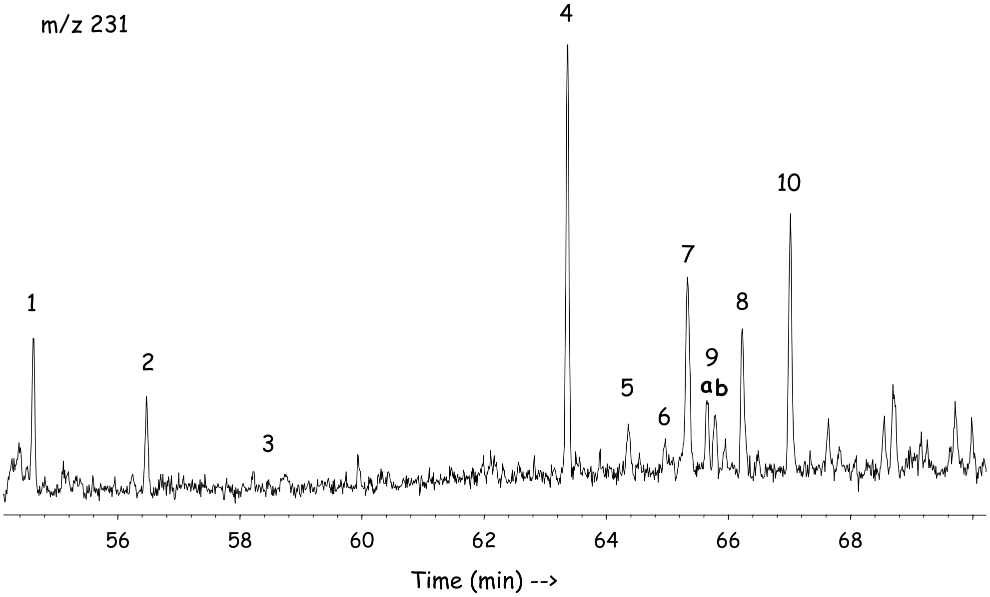

Fig. 9. Mass chromatogram for triaromatic steroids from the aromatic fraction of the Haughton extract. Peak identification is as follows: (1) pregnane; (2) 20-methylpregnane; (3) 20-ethylpregnane; (4) cholestane 20*S*; (5) cholestane 20*R*; (6) stigmastane 20*S*; (7) ergostane 20*R*; (8) stigmastane 20*R*; (9a,b) 24-*n*-propylcholestane 20*S* epimers; (10) 24-*n*-propylcholestane 20*R*.

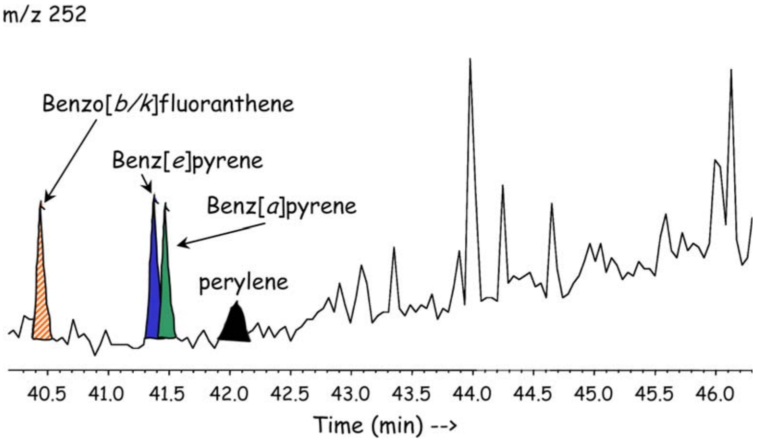

Fig. 10. m/z 252 showing a suite of $C_{20}H_{12}$ PAHs in the Haughton impact structure AH98-2 core extract.

carbons present. These steroids have an unusual distribution (Fig. 9) rich in C_{26} with low relative abundances of C_{27} 20*R* ergostane and no 20*S* ergostane detected. Source input low in C_{28} sterol would, essentially, translate itself by a low expression of C_{27} triaromatic sterols and this is mirrored in the regular sterane contributions in the Haughton extract. Taking cholestane (C_{26}) isomerization the biological 20*R* isomer is depleted relative to the geological 20*S* isomer (Fig. 9; peaks 5 and 4, respectively). These data indicate a higher thermal maturity than that based on C_{28} steroids where the opposite isomerization pattern is true (see Fig. 9; peaks 6 and 8, 20*S* and 20*R* isomers, respectively). This latter isomerization pattern may be a function of source; affected by a higher contribution of C_{29} sterols into the assemblage. A high value of 0.88 for the C_{26} TA 20*S*/(20*S* + 20*R*) ratio indicates a high level of maturity and does not correlate well with maturity proxies obtained from regular steranes but correlates more closely with naphthalene maturity indicators.

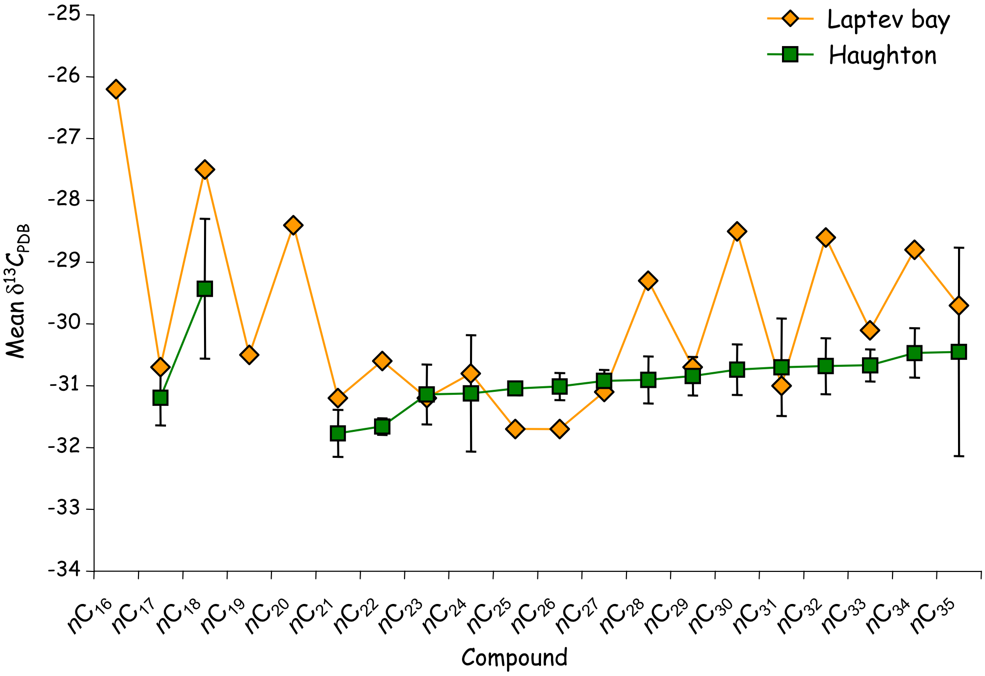

Fig. 11. Comparison of $\delta^{13}C$ compound specific isotope data from Haughton impact structure and Laptev Sea (data published in Zegouagh et al., 1998). Error bars are shown for the Haughton measurements.

Polycyclic aromatic hydrocarbons (PAHs) are present in the Haughton extract (Fig. 10). This suite of PAHs was identified by their mass spectra and retention indices. The dominant PAHs in the extract are the pericondensed aromatic series of phenanthrene, benzo[*e*]pyrene, benzo[*a*]pyrene and perylene. A pyrolytic origin is supported by the presence of the 5-ringed benzofluoranthene. Once this forms it does not easily degenerate to a pericondensed form (Scott, 1982). The lack of alkylated PAHs relative to parent PAHs provides additional evidence to suggest a pyrolytic origin. Since drilling fluids were not used to recover the core, these products are considered derived from natural products.

Dibenzothiophenes (DBT) and methyldibenzothiophenes (MDBT) are both present in the Haughton extract. Data from these compound groups indicate a contribution of organic sulfur to the depositional environment. DBT tend to become amplified relative to MDBT with increased thermal maturity. The ratio DBT/MDBT produces a value of 0.3 and corroborates a thermal maturity approaching a calculated vitrinite reflectance value of 0.7% as derived from the methylphenanthrene index 1, i.e. indicating oil window maturity.

4.5. Carbon isotopes $\delta^{13}C$

Evidence for the origin of organic carbon in the Haughton extract was provided by carbon isotopic ratios for individual hydrocarbons. The δ^{13}C values for C_{16}–C_{22} *n*-alkanes range from −26‰ to −31‰ (Fig. 11). C_{21}–C_{35} *n*-alkanes, within the error of the analysis, do not show significant variation from an average δ^{13}C of −31‰. *n*-Alkanes in oils derived from a common kerogen rarely show δ^{13}C values this consistent for individual *n*-alkanes. This data strongly suggests that the *n*-alkanes in the AH98-3 core extract are derived from a common source.

4.6. Organic petrology

Organic petrology revealed a carbonate rich sample with trace quantities of organic particles. The organic debris is dominated by reworked particles of varying vitrinite reflectance. There is a moderate amount of bitumen impregnation of the pyrite cemented carbonate matrix indicative of mobile extractable bitumen. Vitrinite reflectance measurements of recycled particles ranged 0.38 $\%R_o$ (±0.02)–0.86 $\%R_o$ (±0.05). One particle deemed indigenous has a vitrinite reflectance of 0.23 $\%R_o$. Clearly indigenous organic matter is responsible for minor if any contributions to the extractable organic matter. This implies that most of the biomarkers found in the extractable bitumen are derived from either source generation or has been "picked up" during migration through strata richer in organic detritus.

Table 2a
Parameters used to infer source and depositional environment

Source parameter	
Mean δ^{13}C *n*-alkanes	−31 ± 1.3‰
Sterane index[a]	0.014
Homohopane index[b]	0.11
CPI[c]	1.10
DBT/P	1.56
% C_{27} ββ	22
% C_{28} ββ	17
% C_{29} ββ	60

[a] Steranes/hopanes.

[b] $C_{35}/(C_{31}–C_{35})$ homohopanes.

[c] ((*n*-C23 + 25 + 27 + 29 + 31)/(24 + 26 + 28 + 30 + 32)) + ((*n*-C25 + 27 + 29 + 31 + 33)/(24 + 26 + 28 + 30 + 32)).

5. Discussion

There are several lines of evidence that indicate a complex and multi-source origin for the hydrocarbons in the HIS sample. These sources may include: (a) pyrolysis of a biopolymer, likely post-impact, (b) maturation of organic matter in post-impact fill sediments probably by circulating hydrothermal fluids, (c) geochromatographic extraction by migrating older hydrocarbon fluids that leads us into surmising that there is likely, (d) a contribution from hydrocarbons from deeper Ordovician and/or Cretaceous source rocks. Impact induced brecciation coupled with hydrothermal activity may have provided the energy needed to re-mobilize these older petroleum fluids. Organic petrology and TOC data confirm the Haughton sample hosting the petroleum fluid is itself very lean and incapable of producing the array of compounds found in the extractable bitumen. Hence, the main scenario from this work focuses on fluid migration from Ordovician source rocks. As this fluid migrates through brecciated strata it acquires diagnostic compounds from formations through which it travels. This fluid eventually penetrates the Haughton Formation. Within the formation, the fluid may have once more extracted hydrocarbons borne by deeper organically richer bands, which may represent reworked in-fill, and then migrated further up the sequence to reside in its present location.

5.1. Source and deposition indicators

Table 2a lists ratios used to infer possible precursory organic matter sources and depositional environments for the organic matter at Haughton.

Sources for long-chained *n*-alkanes with little or no carbon predominance may be 2-fold. The CPI (Bray and Evans, 1961) measures the progressive change of long-chain *n*-alkanes during maturation. In recent sediments the major source of long-chain *n*-alkanes is considered to be higher plant waxes. Usually recent sediments would exhibit a strong odd carbon number predominance of *n*-alkanes, but increased thermal maturity results in the loss of predominance. By the peak of oil generation (0.8–1.0 %R_o) little or no predominance is visible. Alternatively, a significant portion of the long-chain *n*-alkanes could derive from other sources such as

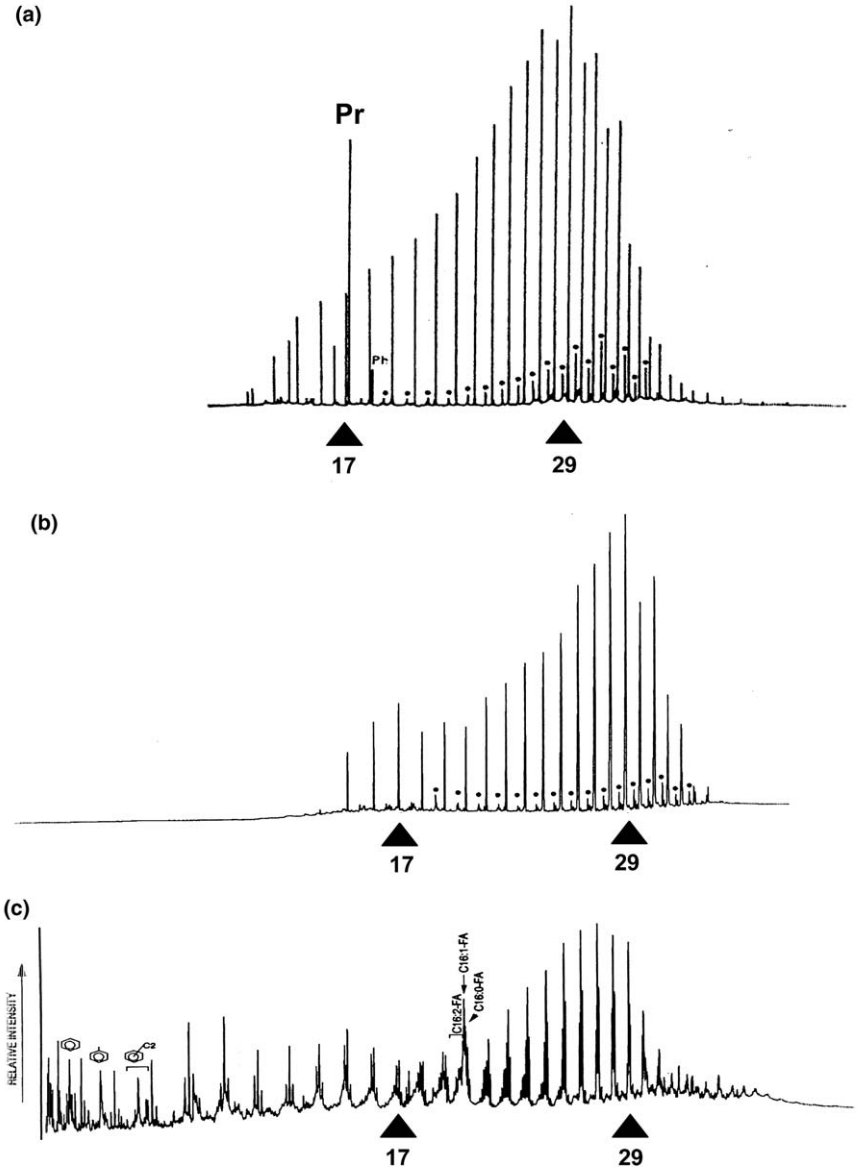

Fig. 12. (a)–(c) Gas chromatogram of the saturated fraction from: (a) *n*-Alkane distributions from a high-wax crude oil from Indonesia. (b) Thermal extract (at 325 °C) of artificially matured highly aliphatic biopolymer of *Agave americana* (circles denote methyl-branched alkanes). (c) TIC of pyrolysate of the intact cuticular membrane of the Upper Miocene fossil gymnosperm *Sciadopitys tertiaria*. Black arrows indicate *n*-alkane retention times (Tegelaar, 1990).

planktonic algae or bacteria (Brocks and Summons, 2003). These organisms produce distributions that do not show carbon predominance even at low levels of thermal maturity. The *n*-alkane distribution of this sample is thought not to be derived from higher plant material, rather it appears more consistent with an algal origin.

Isotope data for the series of *n*-alkanes shows very little variation (±1.3‰) around an average of −31‰. This may represent at least three modes of origin: (a) terrestrial derived organic matter or, (b) algal derived organic matter or, (c) pyrolysis of a highly resistant biopolymer such as algaenan or cutan (Eglinton, 1994; Tegelaar, 1990). Algaenans are highly aliphatic, non-hydrolyzable, and insoluble macromolecules that are consistently found in cell walls of many marine and freshwater green algae (Derenne et al., 1992; Gelin et al., 1996; Blokker et al., 1998). Despite the fact that the precise structure of algaenans still eludes us, clarification with various chemical and thermal degradation techniques suggests that the biopolymers comprise mainly linear, long-chain aliphatic building blocks (Brocks and Summons, 2003) and these are resistant against chemical and biological degradation which leads to their selective preservation during diagenesis (Tegelaar et al., 1989).

Both the *n*-alkane distribution and the isotopic value for each *n*-alkane seem more consistent with an origin from pyrolyzed biopolymeric material such as algaenan or cutan, particularly since when biopolymers are pyrolyzed they yield an *n*-alkane profile that has uniform isotopic compositions (Eglinton, 1994). Figures 12a–c show comparisons for a high-wax crude oil from Indonesia (a) with a thermal extract (at 325 °C) of artificially matured highly aliphatic biopolymer of *Agave Americana* (b) compared with a pyrolysate of the intact cuticular membrane of the Upper Miocene fossil gymnosperm *Sciadopitys tertiaria* (c) (Tegelaar, 1990). These figures bear striking resemblance to the Haughton *n*-alkane profile and suggest that a heating event has affected organic matter at some stage post-impact. Additionally, when biopolymers are pyrolyzed they tend to yield a uniform *n*-alkane distribution with a very slight odd predominance as the biopolymer signal eclipses the odd carbon number predominance from higher plant waxes for example (Tegelaar, 1990).

Comparison of δ^{13}C values from the Lena River Delta and Laptev Sea, Eastern Siberia (Zegouagh et al., 1998) with Haughton shows similar isotopic trends occur in a sample from a bay area (Fig. 11). The isotope values of the Laptev Sea bay sample are attributed to algal lipids. The difference in the two data sets largely lies in the noise surrounding the longer-chain *n*-alkane values. There is much less variability at Haughton. Another scenario is also possible, one where *n*-alkanes are derived from isotopically enriched membrane lipids of food-source mediating bacteria. However, in the context of other data and the lack of variability in the isotopic composition this seems less likely. Thus, the isotopic data is thought to be more consistent with pyrolysis of an aliphatic biopolymer rather than an algal or bacterial lipid origin.

There is a terrestrially derived component at Haughton and this is represented by the diterpenoid hydrocarbons and not the typical biomarkers usually associated with angiosperms and larger-leafed wax-rich plant varieties. The differences in concentration between *n*-alkanes and other compounds indicate that these terrestrial markers may have been either (a) extracted during migration of a Lower Paleozoic fluid, (b) derived from autochthonous flora or (c) allochthonous deposition of formations disrupted by the impact.

Diterpenoid hydrocarbons have been documented to occur in high abundances in the Cretaceous Eureka Sound Group (Kalkreuth et al., 1998). The youngest pre-impact strata of the Eureka Sound Group, however, are found 30 km north of the HIS. Here the group is 210 m thick and rests unconformably on the Silurian rocks (Hickey et al., 1988) of the Grinnell Peninsula (Fig. 1). The Eureka Sound Group dates from Late Cretaceous to Eocene according to Kalkreuth et al. (1998) and Hickey et al. (1988); however, no Eureka Sound Group sediments younger than Late Cretaceous (Maastrichtian) age have been documented on Devon Island (Thorsteinsson and Mayr, 1987). Occurrence of diterpenoid hydrocarbons in the Eureka Sound Group (Kalkreuth et al., 1998) correlates, reasonably closely, with those found in the Haughton Formation during this study. Vegetational reconstruction of the Haughton Formation by Whitlock and Dawson (1990) was based on rich Neogene pollen sediment assemblages. These indicated that indigenous conifer forests with occasional hardwoods covered much of the area. A secondary group of pollen in this assemblage is probably related to the Eureka Sound Group. A third group of pollen remained unidentifiable perhaps due to overmaturity, representative of recycled older material. Indeed, *Pinus* (pine) pollen and other conifer pollens account for 63% of the pollen assemblage. Seven percent of the pollen were pre-Haughton spores and 13% were indeterminable. The diterpenoid record at Haughton seems to mirror these findings, i.e. the assemblage does not represent eroded Eureka Sound Group but extant vegetation that evolved several tens of thousands of years post-impact and became entrained in the lake sediments.

The steranes (C_{29}) and diterpenoid hydrocarbons indicate terrestrially derived organic matter, while biosynthetic pathways for hopanes at Haughton indicate the contribution of at least three biological precursory inputs that seem more closely linked to prokaryotic organisms. Elevated C_{34} homohopane points to a community of bacteria and a possibly anoxic water column, while 2α- and 3α-methylhopanes indicate separate lineages of bacteria. Polycyclic aromatic hydrocarbons indicate a thermal event occurred at Haughton post-impact.

The lack of a structural range of steranes and their low abundances relative to hopanes supports a dominantly prokaryotic precursory input. Conversely, regular steranes seem to represent terrestrial organic matter deposition (Huang and Meinschein, 1979; Moldowan et al., 1985). *n*-24-Propylcholestanes may represent a saline lake rather than a marine depositional environment. During Miocene deposition, Devon Island was elevated above sea level, thereby precluding the possibility of Miocene marine incursions. If this were the case then this would again challenge the premise that the *n*-24-propylcholestanes are solely marine biomarkers (Peters and Moldowan, 1993; Brocks and Summons, 2003). It is more likely, however, that these compounds in the HIS extract emanate from Lower Paleozoic sources that had a contribution from marine algae.

Table 2b
Parameters used to infer thermal maturity

Thermal maturity	
MPI-1	0.47
R_c 0.55 MPI1 + 0.44	0.70
MNR[a]	0.97
C_{26}TA20*S*/(20*S* + 20*R*)	0.88
Ts/(Ts + Tm)[b]	0.51
C30βα hopane/(C30αβ + C30βα)[c]	0.09
C32αβS hopane/(32αβS + 32αβR)[d]	0.60
ααα 20*S* sterane/(20*S* + 20*R*) C_{29}[e]	0.45
αα to ββ C_{29} sterane [f]	0.49

[a] 2-methylnaphthalene/1-methylnaphthalene.

[b] 18α-22,29,30-trisnorneohopane/(18α-22,29,30-trisnorneohopane + 17α-22,29,30-trisnorhopane).

[c] C_{30} 17β,21α(H)-hopane/(17α,21β(H)-hopane + 17β,21α(H)-hopane).

[d] 17α,21β(H)(22*S*)-bishomohopane/(17α,21β(H)(22*S*)-bishomohopane + 17α,21β(H)(22*R*)-bishomohopane).

[e] (29αα*S* + 29ββ*S*)/((29αα*S* + 29ββ*S*) + (29αα*R* + 29ββ*R*)).

[f] (29ββ*R* + 29ββ*S*)/((29ββ*R* + 29ββ*S*) + (29αα*S* + 29αα*R*)).

The prominent presence of MDBT and DBT indicate a depositional environment that was sulfur-rich and probably reducing. Sulfur may have also played a key role in the early release of in situ hydrocarbons. Indeed natural sulfurisation (Sinninghe Damsté et al., 1989, 1995; Köster et al., 1997) (i.e. the reaction of organic matter with reduced inorganic sulfur species during early diagenesis) can be an important diagenetic reaction, modifying the structure and mode of binding of specific biomarkers. This process takes place in the first thousands of years of burial (Werne et al., 2000; Kok et al., 2000). Depending on the structure of the precursor biolipid, biomarker skeletons may in this way be sequestered in higher molecular weight sedimentary organic matter fractions (i.e. via "cross linking" reactions) for millions of years.

5.2. Thermal maturity

Other evidence of hydrocarbon heterogeneity is the subtle disparity in thermal maturity parameters (Table 2b). Sterane 20*S*/(20*S* + 20*R*) has not reached equilibrium with a value of 0.45. The values for the isomerization of ββ/(ββ + αα) C_{29} regular steranes is 0.49 and not at equilibrium. These indicate a lower degree of thermal maturity than maturity parameters from hopanes and methylphenanthrenes (Table 2b). Conversely, aromatic steroids and naphthalenes indicate a higher thermal maturity and may indicate a different provenance for aromatic steroids. Hopane maturity is slightly higher; at least oil window mature. The work of Gentzis et al. (1996) indicates that the underlying Ordovician sedimentary sequence is at a thermal maturity (based on graptolite reflectance) with an equivalent vitrinite reflectance of 0.7%. The methylnaphthalene ratio correlates with the benzothiophene to dibenzothiophenes thermal maturity index and puts thermal maturity in a similar range to the Ordovician, thereby supporting a feasible origin from Ordovician or younger aged source rocks for these compound groups. Solid bitumen from veins and fluid inclusions in carbonates have hopane distributions that include gammacerane, 30-norhopanes (Clark and Philp, 1989) and an *n*-alkane range of shorter carbon chain length with a prominent *n*-C_{17} spike associated with *G. prisca*

(Parnell, personal communication). These have been attributed to an Ordovician source. However, these samples are geochemically distinct from the extract from the Haughton Formation. The hopanes in the Haughton extract and perhaps the C_{30} steranes may indicate origins from a deeper source and that source may indeed be of Ordovician age but may not be related to the Ordovician aged hydrocarbons found in the fluid inclusions and bitumen intrusions from rim structures.

5.3. Evidence for hydrothermal activity

Hydrothermal fluids may have transported enough heat to expel hydrocarbons from more recent sediments and at the same time mobilize deeper sources of hydrocarbons through fracture networks and listric faulting (Whelan et al., 1993). As these fluids migrated they may have encountered dipping basin in-fill strata. Geological evidence indicates that post-impact hydrothermal mineralization is present at Haughton (Osinski et al., 2001). Hydrothermal mineralization sequencing by Osinski et al. (2001) proposed a three-stage model for hydrothermal fluid dissipation and circulation post-impact at Haughton. Phase one impact temperatures may have reached a maximum of 650 °C (based on larnite crystallization) with subsequent rapid cooling. This would have destroyed labile organic matter directly. Eventual cooling to 100 °C is estimated to have occurred over several tens of thousands of years. Fluids in this stage may have been saturated with sulfate ions. Hydrothermal fluids from the latter stages could convert immature sedimentary organic matter to petroleum fluids, which could then migrate upwards, perhaps along listric faults, until they become trapped in a structure or seep to the surface. These fluids may have been mobilized after impact. In contrast to the Jessburger (1988) age of impact of 23 Ma, new ^{40}Ar–^{39}Ar age data (Sherlock et al., personal communication) and field studies (Osinski and Lee, personal communication) place the deposition of the Haughton Formation some 8–10 Ma post-impact, following a considerable erosional event. Hydrothermal activity would, therefore, have ceased to be effectual by this time. Consequently, it seems likely, if this new age data is correct, that material that was hydrothermally heated shortly after impact could have liberated their hydrocarbon load as a result of increased thermal maturity with composite acceleration due to the presence of sulfur. These hydrocarbons may have migrated into the HIS. Alternatively, hydrocarbon source rocks may have been eroded and re-deposited along with extant debris into the Haughton Formation during Miocene times.

The suite of unsubstituted PAHs at Haughton is also a feature that is ubiquitous in higher temperature pyrolysates (Hunt, 1996) and less common in less mature petroleum. This is an important finding that provides further evidence to support (a) biopolymer pyrolysis and (b) the development of a post-impact paleo-hydrothermal fluid system as documented in Osinski et al., 2001. Simoneit (1992) found a similar suite of PAHs in hydrothermal systems in the Escanaba trough and Guaymas basin where hydrothermal systems off the coast of California are currently active. It, therefore, appears that the aromatic hydrocarbons provide more evidence for pyrolysis of sedimentary lipids. However, in order to be consistent with the new ^{40}Ar–^{39}Ar impact dating, these signals are thought to be derived from reworked, hydrothermally altered, sedimentary organic matter.

6. Conclusions

Elucidation of basin architecture via hydrocarbon characterization of a HIS sample reveals a complex history of provenance. The extractable organic solute represents a mixture of hydrocarbons derived from a variety of sources that reflect a unique history for the basin. Moreover, there appear to be distinct groups of compounds that each provide insight to potential sources, depositional environment and thermal evolution. These are (a) *n*-alkanes: pyrolysis of a biopolymer that may have occurred in post-impact in-fill sediments; (b) hopanes, 2α-,3β-methylhopanes: bacterial biomass from a deeper and more mature source of hydrocarbons; (c) homohopane, dibenzothiophenes, benzothiophenes: sulfur-rich depositional environment for the deeper Palaeozoic hydrocarbons; (d) C_{29} steranes and diterpenoids: in situ or low-level reworked terrestrial organic matter; (e) aromatic steroids, *n*-24-propylcholestanes and naphthalenes: again indicating a more mature, deeper seated source; and (f) polycyclic aromatic hydrocarbons such as naphthalenes and phenanthrenes, and *n*-alkanes: indicating the probability that hydrothermal activity and associated elevated temperatures have played an important role during the genesis of the hydrocarbons.

The depositional environment for the deeper seated source appears to be anoxic to sub-oxic and fairly high in sulfur. Particulate organic matter from eroded older formations and extant plant debris has most likely been incorporated into in-fill sediments deposited under a lacustrine depositional environment.

This sample from a Miocene impact crater supports the notion that (a) post-impact erosion and re-sedimentation in a crater lake can create a small and localized source of hydrocarbons and (b) impact-induced brecciation and fracturing coupled with hydrothermal activity has likely caused the re-mobilization of older petroleum fluids. These fluids have migrated into the lake in-fill sedimentary sequence and now rest at their present location pending further migration and/or leakage to the surface or entrapment in a reservoir. This study also demonstrates the complexity of hydrocarbon migration in impact craters.

Acknowledgements

Funding for research conducted at Woods Hole was provided by a grant from the Department of Energy, Basic Energy Sciences to Dr. Jean K. Whelan 113466.04. This manuscript is WHOI contribution number 11279. We thank Dr. Jeff Seewald for valuable comments. We thank the Natural Sciences and Engineering Research Council (NSERC) for grants awarded to M. Douglas. D. Lim was also supported by the following awards: Ontario Graduate Scholarships (OGS), University of Toronto Graduate Studies Fellowships, and the Northern Scientific Training Programme (NSTP). We are particularly indebted to the members of the 1998 HMP crew for recovering and storing core AH98-3, and to Dr. Chris McKay who provided logistical support during our time at NASA Ames Research Center. We would also like to thank Dr. Scott Lamoureux and the EVEX laboratory at Queen's University for their technical support. This is PCSP contribution #04904. Finally, we would like to thank the referees and the Associate Editor for their useful comments and constructive criticism.

Associate Editor—**Martin Koopmans**

References

van Aarssen, B.G.K., Cox, H.C., Hoogendoorn, P., De Leeuw, J.W., 1990. A cadinene biopolymer in fossil and extant dammar resins as a source for cadinanes and bicadinanes in crude oils from southeast Asia. Geochimica et Cosmochimica Acta 54, 3021–3031.

Bishop, A.N., Farrimond, P., Innes, H., Mills, N., 1995. The interpretation and significance of extended hopane distributions (C_{31} to C_{35}) in source rocks and oils. In: Grimalt, J.O., Dorronsoro, C. (Eds.), Organic Geochemistry: Developments and Applications to Energy, Climate, Environment and Human History. A.I.G.O.A, pp. 405–407.

Bisseret, P., Zundel, M., Rohmer, M., 1985. Prokaryotic triterpenoids 2. 2β-methylhopanoids from *Methylobacterium organophilum* and *Nostoc muscorum*, a new series of prokaryotic triterpenoids. European Journal of Biochemistry 150, 29–34.

Blokker, P., Schouten, S., van den Ende, H., de Leeuw, J.W., Hatcher, P.G., Sinninghe Damsté, J.S., 1998. Chemical structure of algaenans from the fresh water algae *Tetraedron minimum*, *Scenedesmus communis* and *Pediastrum boryanum*. Organic Geochemistry 29, 1453–1468.

Bray, E.E., Evans, E.D., 1961. Distribution on *n*-paraffins as a clue to recognition of source beds. Geochimica et Cosmochimica Acta 22, 2–15.

Brocks, J.J., Summons, R.E., 2003. Sedimentary hydrocarbons, biomarkers for early life. In: Holland, H.D. (Ed.), Treatise in Geochemistry, vol. 853. Elsevier, Amsterdam.

Clark, J.P., Philp, R.P., 1989. Geochemical characterization of evaporite and carbonate depositional environments and correlation of associated crude oils in the Black Creek Basin, Alberta. Bulletin of Canadian Petroleum Geology 37, 401–416.

Collister, J.W., Summons, R.E., Lichtfouse, E.L., Hayes, J.M., 1992. An isotopic bio-geochemical study of the Green River oil shale. Organic Geochemistry 19, 265–276.

Derenne, S., Le Berre, F., Largeau, C., Hatcher, P.G., Connan, J., Raynaud, J.-F., 1992. Formation of ultralaminae in marine kerogens via selective preservation of thin resistant outer walls of microalgae. Organic Geochemistry 19, 345–350.

Douglas, A.G., Eglinton, G., Maxwell, J.R., 1969. The organic geochemistry of certain samples from the Scottish Carboniferous formation. Geochimica et Cosmochimica Acta 33, 579–590.

Earth Impact Database, 2004. Available from: http://www.unb.ca/passc/ImpactDatabase/ Accessed: 25 November 2004.

Eglinton, T.I., 1994. Carbon isotopic evidence for the origin of macromolecular aliphatic structures in kerogen. In: Schoell, M., Hayes, J.M. (Eds.), Compound-specific Isotope Analysis in Biogeochemistry and Petroleum Research; Proceedings of a Symposium held at the Spring 1992 National Meeting of the American Chemical Society, San Francisco. Organic Geochemistry, vol. 21, pp. 721–735.

Ekweozor, C.M., Udo, O.T., 1988. The oleananes: origin, maturation, and limits of occurrence in Southern Nigeria sedimentary basins. In: Mattavelli, L., Novelli, L. (Eds.), Advances in Organic Geochemistry 1987, Organic Geochemistry, vol. 13. Pergamon, New York, pp. 131–140.

Farrimond, P., Talbot, H.M., Watson, D.F., Schulz, L.K., Wilhelms, A., 2004. Methylhopanoids: Molecular indicators of ancient bacteria and a petroleum correlation tool. Geochimica et Cosmochimica Acta 68, 3873–3882.

Fowler, M.G., 1984. Organic geochemistry of pre-Carboniferous sedimentary organic matter. Unpublished Ph.D. thesis, The University of Newcastle, England.

Gelin, F., Boogers, I., Noordeloos, A.A.M., Sinninghe Damsté, J.S., de Leeuw, J.W., Hatcher, P.G., 1996. Novel, resistant microalgal polyethers: an important sink of organic carbon in the marine environment. Geochimica et Cosmochimica Acta 60, 1275–1280.

Gentzis, T., de Freitas, T., Goodarzi, F., Melchin, M., Lenz, A., 1996. Thermal maturity of Lower Paleozoic sedimentary successions in Arctic Canada. American Association of Petroleum Geologists Bulletin 80, 1065–1084.

Grieve, R.A.F., Masaytis, V.L., 1994. The economic potential of terrestrial impact craters. International Geological Review 36, 105–151.

ten Haven, H.L., de Leeuw, J.W., Sinninghe Damsté, J.S., Schenck, P.A., Palmer, S.E., Zumberge, J.E., 1988. Application of biological markers in the recognition of palaeohypersaline environments. In: Kelts, K., Fleet, A., Talbot, M. (Eds.), Lacustrine Petroleum Source Rocks. Blackwell, Oxford, pp. 123–130.

Hickey, L.J., Johnson, K.R., Dawson, M.R., 1988. The stratigraphy, sedimentology, and fossils of the Haughton Formation: A post-impact crater-fill, Devon Island, N.W.T., Canada. Meteoritics 23, 221–231.

Huang, W.-Y., Meinschein, W.G., 1979. Sterols as ecological indicators. Geochimica et Cosmochimica Acta 43, 739–745.

Hunt, J.M., 1996. Petroleum Geochemistry and Geology, second ed. W.H. Freeman and Co., New York.

Jessburger, E.K., 1988. ^{40}Ar–^{39}Ar dating of the Haughton impact structure. Meteoritics 23, 233–234.

Kalkreuth, W., Keuser, C., Fowler, M., Li, M., McIntyre, D., Püttmann, W., Richardson, R., 1998. The petrology, organic geochemistry and palynology of Tertiary age Eureka Sound Group coals, Arctic Canada. Organic Geochemistry 29, 799–809.

Kleemann, G., Poralla, K., Englert, G., Kjøsen, H.H., Liaaen-Jensen, S., Neunlist, S., Rohmer, M., 1990. Tetrahymanol from the phototrophic bacterium *Rhodopseudomonas palustris*: First report of a gammacerane triterpene from a prokaryote. Journal of General Microbiology 139, 2551–2553.

Kok, M.D., Schouten, S., Sinninghe Damsté, J.S., 2000. Formation of insoluble, nonhydrolyzable, sulfur-rich macromolecules via incorporation of inorganic sulfur species into algal carbohydrates. Geochimica et Cosmochimica Acta 64, 2689–2699.

Köster, J., Heidy, M.E., van Kaam-Peters, Koopmans, M.P., de Leeuw, J.W., Sinninghe Damsté, J.S., 1997. Sulphurisation of homohopanoids: Effects on carbon number distribution, speciation, and 22S/22R epimer ratios. Geochimica et Cosmochimica Acta 61, 2431–2452.

Largeau, C., Derenne, S., Casadevall, E., Kadouri, A., Sellier, N., 1986. Pyrolysis of immature torbanite and of the resistant biopolymer (PRB A) isolated from extant alga *Botryococcus braunii*. Mechanisms of formation and structure of torbanite. Organic Geochemistry 10, 1023–1032.

Lee, P., Bunch, T.E., Cabrol, N., Cockell, C.S., Grieve, R.A.F., McKay, C.P., Rice, J.W. Jr., Schutt, J.W., Zent, A.P., 1998. Haughton-Mars 97–In: Overview of Observations at the Haughton Impact Crater, a Unique Mars Analog Site in the Canadian High Arctic (abstract). 29th Lunar and Planetary Science Conference, 1973–1974.

Lim, D.S.S., 2004. Limnology and diatom paleoecology of lakes and ponds on Banks Island, N.W.T. and Devon Island, Nunavut, Canadian Arctic. Ph.D. thesis, University of Toronto, Canada.

Mackenzie, A.S., 1980. Unpublished Ph.D. thesis, University of Bristol, England.

Mackenzie, A.S., Application of biomarkers in petroleum geochemistry, 1984. In: Brooks, J., Welte, D.H. (Eds.), Advances in Petroleum Geochemistry, vol. 1. Academic Press, London, pp. 115–214.

Mazur, M.J., Stewart, R.R., Hildebrand, A.R., 2000. The seismic signature of meteorite impact craters. Canadian Society of Exploration Geophysicists Recorder (June), 10–16.

Moldowan, J.M., Seifert, W.K., Gallegos, E.J., 1985. Relationship between petroleum composition and depositional environment of petroleum source rocks. American Association of Petroleum Geologists Bulletin 69, 1255–1268.

Moldowan, J.M., Fago, F.J., Lee, C.Y., Jacobson, S.R., Watt, D.S., Slougui, N.E., Jeganathan, A., Young, D.C., 1990. Sedimentary 24-*n*-propylcholestanes, molecular fossils diagnostic of marine algae. Science 247, 309–312.

Osinski, G.R., Spray, J.G., 2001. Impact-generated carbonate melts: evidence from the Haughton structure, Canada. Earth and Planetary Science Letters 194, 17–29.

Osinski, G.R., Spray, J.G., 2003. Evidence for the shock melting of sulfates from the Haughton impact structure, Arctic Canada. Earth and Planetary Science Letters 215, 357–370.

Osinski, G.R., Spray, J.G., Lee, P., 2001. Impact-induced hydrothermal activity within the Haughton impact structure, arctic Canada: Generation of a transient, warm, wet oasis. Meteoritics and Planetary Science 36, 731–745.

Otto, A., Simoneit, B.R.T., 2001. Chemosystematics and diagenesis of terpenoids in fossil conifer species and sediment from Eocene Zeitz formation, Saxony, Germany. Geochimica et Cosmochimica Acta 65, 3505–3527.

Otto, A., Simoneit, B.R.T., 2002. Biomarkers of Holocene buried conifer logs from Bella Coola and North Vancouver, British Columbia, Canada. Organic Geochemistry 33, 1241–1251.

Otto, A., Wilde, V., 2001. Sesqui-, di-, and triterpenoids as chemosystematic markers in extant conifers – A review. Botanical Review 67, 141–238.

Otto, A., Walther, H., Püttmann, W., 1997. Sesqui- and diterpenoid biomarkers preserved in Taxodium-rich Oligocene oxbow lake clays, Weisselster basin, Germany. Organic Geochemistry 26, 105–115.

Pancost, R.D., Freeman, K.H., Patzkowsky, M.E., Wavrek, D.A., Collister, J.W., 1998. Molecular indicators of redox and marine photoautotroph composition in the late Middle Ordovician of Iowa, USA. Organic Geochemistry 29, 1649–1662.

Parnell, J., Osinski, G.R., Lee, P., Baron, M., Pearson, M.J., Feely, M., 2003. Hydrocarbons in the Haughton Impact Structure Devon Island, Nunavut, Canada. Lunar and Planetary Science XXXIV, pp. 1118.

Peters, K.E., Moldowan, J.M., 1991. Effects of source, thermal maturity, and biodegradation on the distribution and isomerization of homohopanes in petroleum. Organic Geochemistry 17, 47–61.

Peters, K.E., Moldowan, J.M., 1993. The Biomarker Guide: Interpreting Molecular Fossils in Petroleum and Ancient Sediments. Prentice Hall, Englewood Cliffs, NJ.

Peters, K.E., Moldowan, J.M., McCaffrey, M.A., Fago, F.J., 1996. Selective biodegradation of extended hopanes to 25-norhopanes in petroleum reservoirs. Insights from molecular mechanics. Organic Geochemistry 24, 765–783.

Philp, R.P., 1985. Fossil Fuel Biomarkers Applications and Spectra. Methods in Geochemistry and Geophysics, 23. Elsevier Science, Amsterdam.

Radke, M., 1988. Application of aromatic compounds as maturity indicators in source rocks and crude oils. Marine and Petroleum Geology 5, 224–236.

Radke, M., Welte, D.H., 1983. The methylphenanthrene index (MPI); a maturity parameter based on aromatic hydrocarbons. In: Bjorøy, M., et al. (Eds.), Advances in Organic Geochemistry, 1981, Proceedings of the International Meeting on Organic Geochemistry. Wiley and Sons, New York, pp. 504–512.

Radke, M., Welte, D.H., Willsch, H., 1982. Geochemical study on a well in the western Canada Basin; relation of the aromatic distribution pattern to maturity of organic matter. Geochimica et Cosmochimica Acta 46, 1–10.

Radke, M., Willsch, H., Teichmueller, M., 1990. Generation and distribution of aromatic hydrocarbons in coals of low rank. Organic Geochemistry 15, 539–563.

Redeker, H.J., Stöffler, D., 1988. The allochthonous polymict breccia layer of the Haughton impact crater, Devon Island, Canada. Meteoritics 23, 185–196.

Robertson, P.B., 1988. The Haughton Impact Structure, Devon Island, Canada: Setting and history of investigations. Meteoritics 23, 181–184.

Robinson, N., Brassell, S., Parnell, J., 1989. Hydrocarbon compositions of bitumens from mineralized Devonian lavas and Carboniferous sedimentary rocks, central Scotland. Marine and Petroleum Geology 6, 316–323.

Rohmer, M., 1987. The hopanoids, prokaryotic and sterol surrogates. In: Schriner, E. et al., (Eds.), Surface Structures of Microorganisms and their Interactions with the Mammalian Host, Proceedings of the 18th Workshop Conference, Hocchst, Schloss Ringberg, October 20-13, 1987. VCH, pp. 227–242.

Schoell, M., Hwang, R.J., Carlson, R.M.K., Welton, J.E., 1994. Carbon isotopic composition of individual biomarkers in gilsonites (Utah). In: Schoell, M., Hayes J.M. (Eds.), Compound-Specific Analysis in Biogeochemistry and Petroleum Research; Organic Geochemistry, vol. 21, pp. 673–683.

Schutt, J., Dunfield, G., Grin, E., Lee, P., Reyes, D., 2002. DRILLEX The Drilling experiment at Haughton Crater, Nunavut, Canada. For more information see http://resources.yesican.yorku.ca/trek/mars/classroom/drillex.htm.

Scott, L.T., 1982. Thermal rearrangements of aromatic compounds. Accounts of Chemical Research 15, 52–58.

Seifert, W.K., Moldowan, J.M., 1980. The effect of thermal stress on source rock quality as measured by hopanes stereochemistry. In: Douglas, A.G., Maxwell, J.R. (Eds.), Advances in Organic Geochemistry 1979. Pergamon, New York, pp. 229–237.

Shimoyama, A., Hagiwara, M., Nomoto, S., 2000. Naphthalenes in Neogene sediments of the Shinjo basin, Japan. Geochemical Journal 34, 333–340.

Simoneit, B.R.T., 1992. Natural hydrous pyrolysis: Petroleum generation in submarine hydrothermal systems. In: Whelan, J., Farrington, J.W. (Eds.), Organic Matter: Productivity, Accumulation and Preservation in Recent and Ancient Sediments. Columbia University Press, New York.

Sinninghe Damsté, J.S., Rijpstra, W.I.C., de Leeuw, J.W., Schenck, P.A., 1989. The occurrence and identification of series of organic sulphur compounds in oils and sediment extracts: II. Their presence in samples from hypersaline and non-hypersaline palaeoenvironments and possible application as source, palaeoenvironmental and maturity indicators. Geochimica et Cosmochimica Acta 53, 1323–1341.

Sinninghe Damsté, J.S., Kenig, F., Koopmans, M.P., Köster, J., Schouten, S., Hayes, J.M., de Leeuw, J.W., 1995. Evidence for gammacerane as an indicator of water column stratification. Geochimica et Cosmochimica Acta 59, 1895–1900.

Strachan, M.G., Alexander, R., Kagi, R.I., 1988. Trimethylnaphthalenes in crude oils and sediments: Effects of source and maturity. Geochimica et Cosmochimica Acta 52, 1255–1264.

Sukh Dev, 1989. Terpenoids. In: Rowe, J.W. (Ed.), Natural Products of Woody Plants, vol. 1. Springer, Berlin, pp. 691–807.

Summons, R.E., Jahnke, L.L., 1992. Hopenes and hopanes methylated in ring-A: correlation of the hopanoids of extant methylotrophic bacteria with the fossil analogues. In: Moldowan, J.M., Albrecht, P., Philp, R.P. (Eds.), Biomarkers in Sediments and Petroleum. Prentice Hall, Englewood Cliffs, NJ, pp. 182–200.

Summons, R.E., Jahnke, L.L., Simoneit, B.R.T., 1996. Lipid biomarkers for bacterial systems: studies of cultured organisms, hydrothermal environments and ancient sediments. In: Bock, G.R., Goode, J.A. (Eds.), Evolution of Hydrothermal Ecosystems on Earth (and Mars?). Wiley, Chichester (Ciba Foundation Symposium 202), pp. 174–194.

Summons, R.E., Jahnke, L.L., Hope, J.M., Logan, G.A., 1999. 2-Methylhopanoids as biomarkers for cyanobacterial oxygenic photosynthesis. Nature 400, 554–557.

Tegelaar, E.W., 1990. Resistant biomacromolecules in morphologically characterized constituents of kerogen: A key to the relationship between biomass and fossil fuels. Ph.D. thesis, University of Utrecht, The Netherlands.

Tegelaar, E.W., de Leeuw, J.W., Derenne, S., Largeau, C., 1989. A reappraisal of kerogen formation. Geochimica et Cosmochimica Acta 53, 3103–3106.

Thomas, B.R., 1970. Modern and fossil plant resins. In: Harborne, J.B. (Ed.), Phytochemical Phylogeny. Academic Press, London, pp. 59–79.

Thorsteinsson, R., Mayr, U., 1987. The Sedimentary Rocks of Devon Island, Canadian Arctic Archipelago. Geological Survey of Canada – Memoir 411, pp. 182.

Werne, J.P., Hollander, D.J., Behrens, A., Schaeffer, P., Albrecht, P., Sinninghe Damsté, J.S., 2000. Timing of early diagenetic sulfurization of organic matter: a precursor-product relationship in Holocene sediments of the anoxic Cariaco Basin, Venezuela. Geochimica et Cosmochimica Acta 64, 1741–1751.

Whelan, J.K., Kennicutt II., M.C., Brooks, J.M., Schumacher, D., Eglinton, L.B., 1993. Organic geochemical indicators of dynamic fluid flow processes in petroleum basins. Organic Geochemistry 22, 587–615.

Whitlock, C., Dawson, M.R., 1990. Pollen and vertebrates of the Early Neogene Haughton Formation, Devon Island, Arctic Canada. Arctic 43, 324–330.

Zegouagh, Y., Derenne, S., Largeau, C., Bardoux, G., Mariotti, A., 1998. Organic matter sources and early diagenetic alterations in Arctic Surface Sediments (Lena River Delta and Laptev Sea, Eastern Siberia), II. Molecular and isotopic studies of hydrocarbons. Organic Geochemistry 28, 571–583.

Zundel, M., Rohmer, M., 1985a. Hopanoids of the methylotrophic bacteria *Methylococcus capsulatus* and *Methylomonas* sp. as possible precursors for the C_{29} and C_{30} hopanoid chemical fossils. Federation of European Microbiological Societies Microbiology Letters 28, 61–64.

Zundel, M., Rohmer, M., 1985b. Prokaryotic triterpenoids 1. 3-methylhopanoids from *Acetobacter* sp. and *Methylococcus capsulatus*. European Journal of Biochemistry 150, 23–27.

Zundel, M., Rohmer, M., 1985c. Prokaryotic triterpenoids 3. The biosynthesis of 2β-methylhopanoids and 3β-methylhopanoids of *Methylobacterium organophilum* and *Acetobacter pasteurianus* spp. *pasteurianus*. European Journal of Biochemistry 150, 35–39.